Scanning Microscopy

Volume 2 | Number 1 Article 54

7-13-1987

Scanning Electron Microscopy of Vertebrate Cerebellar Cortex

Orlando J. Castejón
Universidad del Zulia

Scanning Microscopy, Vol. 2, No. 1, 1988 (Pages 569-597)
Scanning Microscopy International, Chicago (AMF O'Hare), IL 60666 USA

0891-7035/88$3.00+.00

SCANNING ELECTRON MICROSCOPY OF VERTEBRATE CEREBELLAR CORTEX

Orlando J. Castejón

Instituto de Investigaciones Biológicas
Facultad de Medicina
Universidad del Zulia
Apartado Postal 526
Maracaibo, Venezuela

(Received for publication March 10, 1987, and in revised form July 13, 1987)

Abstract

In this study, the Golgi method for light microscopy, transmission and conventional scanning electron microscopy, the ethanol-cryofracturing technique, the freeze-fracture method for SEM, and the freeze-etching method have been used in conjunction to analyze the three-dimensional cytoarchitectonic arrangement and intracortical circuits of vertebrate cerebellar cortex. Approximately more than 100 specimens of mice, rat, teleost fishes and human cerebelli were processed by the above mentioned techniques. A chronological review of other methods for studying hidden surfaces of cerebellar nerve cell has been also described. The three-dimensional morphology, outer and inner surfaces of granule, Golgi, Purkinje and stellate cells were reviewed by means of a correlative and comparative study. The cerebellar circuits formed by mossy and climbing fibers with granule cell dendrites and Purkinje cell-granule cell synapses have been traced by ethanol-cryofracturing technique, freeze-fracture method for SEM and freeze-etching technique. These findings have been correlated with previous light and electron microscope findings published in the last century. Some advantages and limitations of each method are pointed out. The review emphasizes the paramount importance of correlating light microscope Golgi method with ethanol-cryofracturing and slicing techniques for SEM. The correlation between freeze-fracture method for SEM and freeze-etching technique provides a new approach for studying three-dimensional morphology of nerve cells at cellular and macromolecular levels. This modern methodology of three-dimensional analysis offers new potential areas for future experimental investigation in embryology and pathology of the central nervous system.

KEY WORDS: Scanning Electron Microscopy, Cerebellum, Freeze-Etching, Neurons, Synapses, Teleost Fishes.

* Address for correspondence:
O.J. Castejón. Instituto de Investigaciones Biológicas. Facultad de Medicina. Universidad del Zulia. Apartado Postal 526. Maracaibo, Venezuela.
phone number: 58-61 911772

Introduction

Before the advent of scanning electron microscopy, the problem of three-dimensional organization of nerve cells was mainly approached through the laborious reconstruction techniques of light and transmission electron microscopic serial sectioning, isolation of individual neurons, tissue cultures, neurohistological techniques (particularly the Golgi method), intracellular staining and computer assisted methods (see review of Mannen, 1978).

The classical neurohistological techniques for light microscopy reveal only an incomplete cellular outline or silhouette and little internal details of neurons and neuroglial cells. The images produced by light microscope are informative but limited in resolution. Transmission electron microscopy (TEM) on the contrary, provides a full range of high resolution information on cellular organization in faithful details within the restricted field of a thin section but lacks the three-dimensional representation of tissue organization.

The scanning electron microscope (SEM) offers the unique possibility of displaying in three-dimensions, the remarkable complexity of nerve cell organization and interrelationship in situ. In addition, SEM provides the capacity to scan relatively large areas of brain parenchyma with relatively high resolution and depth of focus.

Progress in the development and application of biological techniques in SEM during the last three decades has resulted in a marked increase in our knowledge and comprehension of the organization of nerve tissue. A number of investigations have been published that have attempted to reveal by SEM, the three-dimensional cellular organization of different regions of the central nervous system (CNS) (Boyde and Wood, 1969; Hansson, 1970; Lewis, 1971; Obtsuki, 1972; Krstic, 1974; Phillips et al., 1974; Saetersdal and Myklebust, 1975; Estable-Puig and Estable-Puig, 1975; Seymour and Berry, 1975; Tanaka et al., 1976; Lametschwandtner et al., 1977; Antal, 1977; Fasekas et al., 1978; Hartwig and Korf, 1978; Bredberg, 1979; Merchant, 1979; Siew, 1979; Kessel and Kardon, 1981; Matsuda and Uehara, 1981; Low, 1982; Eagleson and Malacinski, 1986).

The cerebellar cortex is a well studied,

highly organized region of the brain containing five closely packed major neuronal types, stratified in three geometrically arranged layers. Their compact disposition has limited the early application of SEM, since this methodology was initially specifically developed for surface observations (see review of Mitchell, 1980). Therefore, earlier observations were confined to cerebellar cultures (Privat et al., 1973; Silberberg, 1975; Messer, 1977). Lately, several methods have been designed in order to facilitate SEM study of cerebellar nerve cells hidden surfaces or structures not readily accessible at the level of gray and white cerebellar matter (Lewis, 1971; Castejón et al., 1976; Castejón and Caraballo, 1980a, b; Castejón and Valero, 1980; Castejón, 1981, 1983, 1984, 1986; Castejón and Castejón, 1981, 1987; Scheibel et al., 1981; Arnett and Low,1985). These methods currently being used to study the three-dimensional organization of vertebrate cerebellar cortex are the results of independent research projects carried out in a number of laboratories over the past fifteen years. Each method provides a somewhat similar view of the layers of the cerebellar cortex, and each has its own advantages and limitations. Fortunately, the information that can be obtained by the different methods is complementary, so that it is potentially possible to make up for the limitations of one method by using one of the others.

The aim of the present paper is to review the SEM methods applied to the study of vertebrate cerebellum, putting special emphasis on the cytoarchitectural arrangement and intracortical neuronal circuits.

Chronological Review of SEM Methods for Studying Three-Dimensional Organization of Cerebellar Cortex

The low temperature dry ashing technique (Lewis, 1971).

The silver-stained nervous tissue of cat, sectioned or unsectioned, is placed in a flowing oxygen plasma generated by a 13.56 MHz radio-frequency field in a commercial (Trapelo) low temperature asher. The pressure of the activated gas is approximately 100mm, and its flow rate generally is adjusted to 100cc per minute. The power delivered to the plasma is continuously controllable, from approximately 2 watts. 10µm sections can be ashed thoroughly in less than 2h. In the ashing process, organic matter (containing C, H, O, N, S) is oxidized and thus volatilized (as CO_2, H_2O, SO_2 and N_2 or oxides of N) in the low pressure plasma while inorganic material remains behind. With this technique the silver precipitate could become a neuronal replica for SEM. Granule cells, Purkinje and molecular layers were clearly distinguished and the nerve cells generally displayed a reasonably intact surface. The process of ashing did not noticeably alter the integrity of cerebellar cortex.

Slicing technique for SEM (Castejón and Caraballo, 1980a).

Specimens of Arius spixii weighing 30-82g, kept in aquaria at room temperature were used. Pieces of tissue were fixed: 1) by immersion in 5% glutaraldehyde in 0.1M phosphate buffer, pH 7.4; or 2) by vascular perfusion with 4% glutaraldehyde in 0.1M phosphate buffer solution, pH 7.4; or 3) by immersion with the Karnovsky fixative. Slices of 2-3mm thick were cut with a razor blade and fixed overnight in the same buffered fixative. After washing in buffered saline, the tissue blocks were dehydrated through graded concentrations of ethanol, dried by the critical point method with liquid CO_2 as recommended by Anderson (1951), mounted on copper stubs and coated with carbon and gold-palladium. The specimens were examined in a JEOL 100B Electron Microscope with ASID scanning attachment at 20 kV.

Ethanol-Cryofractography applied to human cerebellum (Castejón and Caraballo, 1980b).

This technique originally designed by Humphreys et al. (1975) to scan liver and kidney tissue was applied by us to study only human cerebellar cortex. The samples 3-5mm thick were fixed for 2 to 16h in 4% glutaraldehyde-phosphate buffer solution, 0.1M, pH 7.4, dehydrated in ethanol and frozen in liquid nitrogen. The fracture was made with a precooled razor blade and the fragments placed in ethanol at room temperature for thawing. The critical point drying was done with liquid CO_2 followed by a coating of carbon or gold-palladium in a JEOL-46 high vacuum evaporator. The tissue was observed with a JEM 100B EM-ASID.

The "creative tearing" technique (Scheibel, et al., 1981).

The cerebellar neuropil of Mongolian gerbil, rat, cat, monkey and human, is revealed by careful tearing of aldehyde-fixed tissue specimens, which were prepared by means of dehydration, critical point freeze-drying and sputter-coating with gold-palladium. The authors applied a modified free-hand dissection to the tissue. After determining the desired plane of cleavage, a small cut with scalpel or razor was made in a corner of the tissue block. Using the incision as the starting point, the tissue was slowly torn in the plane already established. The method followed the natural cleavage planes within the tissue. The technique provided a remarkable three-dimensional view of neuropil including cell bodies and dendrites, details of pre- and postsynaptic morphology, axonal structure, neuroglia and the microvasculature.

Freeze-fracture SEM method (Castejón, 1981).

This method was applied to study the cerebellar cortex of two teleost fishes: Arius spixii and Salmo trout. After Karnovsky fixation, cerebellar slices, 2-3mm thick, were cut with a razor blade and fixed by immersion in the same fixative for 4-5h. After washing in buffered saline, they were postfixed in 1% osmium tetroxide in 0.1M phosphate buffer solution, pH 7.4 for 1h. After rinsing in a similar buffer, tissue blocks were dehydrated through graded concentrations of ethanol, rapidly frozen by plunging into Freon 22, cooled by liquid nitrogen (Haggis, 1970; Haggis and Phipps-Todd, 1977) and fractured with a precooled razor blade. The fracture fragments were returned to fresh absolute ethanol for thawing. According to Haggis et al., in the FDFf method, the cytoplasmic and nuclear soluble proteins are washed out, presumably during the thawing step, leaving anfractuous cavities surrounding the cytomembranes and allowing visualization of the surface details of cytoplasmic and nuclear structures. The tissue was then dried by the critical point method with liquid CO_2 as recommended by Anderson (1951) and coated with gold-palladium. Specimens were examined in a JEOL 100B EM-ASID scanning attachment at 80 kV.

Cryoprotected freeze-fractured SEM (Castejón, 1983).

The cerebelli of mice and rats were dissected out from animals under anesthesia and immersed in 0.1M buffered phosphate-glutaraldehyde fixative solution and postfixed in a similar buffered osmium tetroxide solution. After washing, half of the tissues were dehydrated in absolute ethanol, and of the remainder, about one third were slowly brought to 50% glycerol in distilled water and the rest slowly brought to 50% DMSO in distilled water. The tissues in absolute ethanol were then divided and some were rapidly frozen by plunging into Freon 22 held at -150°C with liquid nitrogen. Others were frozen at medium freezing rate by plunging directly into liquid nitrogen. Under liquid nitrogen these tissues were fractured with a precooled razor blade. The tissues in 50% glycerol and 50% DMSO were rapidly frozen, fractured under liquid nitrogen and rewarmed in the 50% glycerol and 50% DMSO solutions, respectively. All glycerol and DMSO treated samples were subsequently dehydrated in absolute ethanol and all samples were critical point dried from ethanol, then gold-palladium coated for SEM viewing.

Ultrasonic microdissection (Arnett and Low, 1985).

Rat cerebellar samples were initially fixed with aldehydes. Blocks of tissue were razor cut and treated by three separate methods: 1) Immersion in 1% aqueous boric acid or 2) in 2% phosphate buffered OsO_4 followed by boric acid or 3) in an 8/2 mixture of boric acid and OsO_4. After 18-48h of immersion the blocks were dehydrated and exposed to ultrasonic in 100% acetone at frequencies of 80 kHz for 10 to 20 minutes. Specimens were then critical-point dried using liquid CO_2, mounted on SEM stubs and sputter-coated with gold-palladium. Microdissection of cut surfaces (erosion) occurred after all three treatments. With this technique all cerebellar cell types were recognizable. The neuronal processes and some synaptic relationships in the granular layer were distinguished.

Complementary and Correlative Techniques

In addition to the SEM methods above mentioned, we have used the following correlative methods: 1) Golgi light microscopy (Castejón, 1981): Fragments of Swiss albino mouse and teleost fish (Arius spixii) cerebellar cortex, 5-10mm thick, were processed according to the rapid Golgi method (Cajal and De Castro, 1972). Sagittal and transverse sections of the cerebellar cortex, 50-70µm thick, were observed in a Zeiss II Photomicroscope using X 25 and X 40 objectives. 2) Light microscopy of plastic embedded material (Castejón and Caraballo, 1980a): The brains of Swiss albino mice and teleost fishes (Arius spixii) were removed and the cerebellar samples were fixed immediately by immersion in 4% glutaraldehyde in 0.1M phosphate buffer solution, pH 7.4 for 4-16h at 4°C; postfixed for 1h in a similarly buffered 1% osmium tetroxide solution, dehydrated through graded concentrations of ethanol and embedded in Araldite. Thick sections 1-1.5µm, obtained with an LKB Pyramitome equipped with a glass knife, were stained with toluidine blue and observed with a Zeiss II Photomicroscope. 3) Transmission electron microscopy (Castejón and Caraballo, 1980b): For transmission electron microscopy (TEM), slices 1-2mm thick of fish and mouse cerebellar cortex were immediately fixed by immersion in 4% glutaraldehyde in 0.1M phosphate buffer solution, pH 7.4, for 4-16h at 4°C; postfixed for 1h in a similarly buffered 1% osmium tetroxide, dehydrated through graded concentrations of ethanol and embedded in Araldite. Thin sections were stained with uranyl and lead salts and observed with a Siemens Elmiskop I and JEOL 100B electron microscopes. 4) Freeze-etching and direct replicas (Castejón, 1984): This technique was applied to the cerebellar cortex of adult Swiss albino mice. The brains were carefully removed and thin 1-2mm slices of the cerebellar cortex were fixed in 1% ice-cold glutaraldehyde 0.1M phosphate buffer, pH 7.2-7.4, for 1h. All cut pieces were immersed in three changes of 25% glycerol in a similar buffer for periods of 1/2h, mounted on gold discs and frozen in Freon at liquid N_2 temperature for 3-5 seconds. They were immediately transferred to a Balzer BAF-301 freeze-fracture unit equipped with an electron beam gun, at -110°C, in a vacuum of 4×10^{-6} or better. Fractured surfaces were shadowed with a layer of carbon-platinum of about 2.5nm thick. Replicas were floated off on water, cleaned in Chlorox overnight, rinsed in H_2O, bathed in 50% H_2SO_4 and rinsed in multiple changes of water. Cleaned replicas were mounted on grids usually coated with parlodion or Formvar films, and examined with a JEOL 100B electron microscope.

More than 100 specimens of mice, rats, teleost fishes (Arius spixii, Salmo trout) and human cerebelli were used by us for SEM and complementary techniques.

Results

The present review gives a detailed report of the results obtained in vertebrate cerebellum when SEM and complementary techniques were applied. The white and gray matter (granular, Purkinje and molecular layers) are successively described.

Cerebellar White Matter.

In the white matter of the teleostean cerebelli examined by light microscopy, bundles of myelinated axons (Fig. 1), formed by the afferent fibers (climbing and mossy fibers) and the efferent Purkinje cell axons were seen. The low resolution of the light microscope does not allow the characterization of the distinctive features of these myelinated axonal processes. In rat cerebellar folia examined by SEM at very low magnification, in a plane parallel to their main longitudinal axis, cerebellar afferent fibers appeared running longitudinally following the main axis of white matter (Fig. 2). At the apex of the folia, both mossy and climbing fibers followed an approximately radial course from the white matter to the granular layer, supporting the Golgi-light microscope description of O'Leary et al. (1968). At higher magnification (Fig. 3), the different caliber of the mossy and climbing fibers was clearly seen. Mossy fibers could be identified as thick axons following an almost straight course while the climbing fibers were distinguished as fine, wavy processes. These findings, as pointed out by Mugnaini (1972), support the concept that climbing fibers in light microscopy are usually thinner than mossy fibers. A climbing fiber-mossy fiber proportion rate of 5 to 1 could be roughly estimated.

Cerebellar Gray Matter.

Light microscope examinations of vertebrate

cerebellar gray matter reveal a three layered structure: granular, Purkinje and molecular layers (Fig. 4). This regular histological organization, apparent simplicity and beautiful geometrical arrangement is extraordinarily well suited for comparative three-dimensional studies. In some teleostean fish cerebellum (Arius spixii) we have, in addition, described a fourth layer: the fibrous stratum (Castejón and Caraballo, 1980a), mainly composed by compact bundles of myelinated axons located between the Purkinje and granular layers (Fig. 5).

Granule cell layer. In this layer, the granule cell features, mossy and climbing fiber glomeruli, and the Golgi cell organization are described.

Granule cells. At the light microscope level, the granule cells stained with toluidine blue are seen forming groups of approximately 7-12 cells, separated by clear spaces corresponding to the glomerular regions or by the Golgi cells (Fig. 6). Capillaries and bundles of myelinated axons also separate the granule cell clusters.

An almost complete view of the cytoarchitectonic organization of fish cerebellar cortex could be appreciated at SEM level low magnification using the slicing technique (Fig. 7). A reliable identification of granule and Purkinje cells could be assured, while the complex intracortical network formed by undifferentiated afferent and intrinsic fibers was also seen with this technique. The granule neurons appeared either as smooth surfaced spheroidal cells arranged like bunches of grapes or as isolated randomly distributed cells. The granule cell dendrites (Fig. 8) emerged from the cell body in a pyramidal shape and could be traced to the neighboring granule cells or the nearest glomerulus. These dendrites two to four in number, followed an unbranched, wavy course and ended in a triangular shaped terminal dendritic claw which appeared in contact with the mossy fiber rosette at the level of the glomerular region. The filiform granule cell axon, originating directly from the cell body, was comparatively more slender than the dendritic processes. It was observed ascending to the molecular layer to synapse with Purkinje dendritic arborization. The SEM freeze-fracture method applied to Salmo trout cerebellum revealed closely packed granule cells (Fig. 9), whose plasma membranes appeared to be in intimate apposition. The fracture passed across the equatorial plane of cell somata allowing us to visualize the outer surface of the nucleus, held in a central or peripheral position by some cytoplasmic strands. These fine fibrils running from the nuclear outer surface to the inner surface of the plasma membrane formed a cytoplasmic network in which cell organelles (mitochondria, lysosomes) were suspended. The arrangement and disposition of these cytoplasmic strands correspond to the distribution of granule cell endoplasmic reticulum. The cytoplasmic strands exhibited small or medium size varicosities or globular enlargements which apparently correspond to the cisterns and vesicles of endoplasmic reticulum. The rest of the cytoplasm appeared almost empty. The freeze-fracture method washes out the soluble proteins of cytoplasmic matrix creating the three-dimensional view of the granule cell interior. Samples of teleost fish (Arius spixii) processed by the SEM freeze-fracture method (Fig. 10) showed fractured granule cells, in which the nuclear chromatin and the outer surface of the endoplasmic reticulum were observed. This image could be well correlated with the TEM appearance of granule cell morphology (Castejón, 1969, 1981, 1984; Palay and Chan-Palay, 1974).

Freeze-etching replicas of mouse fractured granule cells (Fig.11) showed the thin rim of perikaryal cytoplasm and the P face plasma membrane, which exhibited randomly dispersed intramembrane particles. The fractured spheroidal nucleus displayed the P face inner nuclear membrane, the E face outer nuclear membrane and the nuclear pores. The cytoplasmic fracture face bearing scarce endoplasmic reticular profiles was also observed.

Mossy fiber glomerulus. With the slicing technique for SEM the morphology of teleost fish glomerular regions could be properly studied. At the granular layer, the characteristically thick mossy fibers (Fig. 12) arborized dichotomously, originating thinner secondary branches, while on the contrary, the climbing fibers pursued a curvaceous course and a typical cross-over bifurcation pattern or arborescence pattern type of bifurcation characteristically spreading thin collaterals in three different planes. The mossy fibers generally remain in the granular layer while the climbing fibers continue their course ascending to the Purkinje cell layer. The mossy glomerular regions (Fig. 13) appeared as entangled threads, polygonal, round or ovoid in shape, formed by the convergence of dendritic processes of many granule and Golgi cells upon the fiber rosette. In fact, the mossy fiber enters into the clew and appears surrounded

Fig. 1. Photomicrograph of teleost fish (Arius spixii) cerebellar cortex. Section passing through white matter (WM) of the cerebellar cortex, showing the entry of extrinsic fibers (mossy and climbing fibers) into the granular layer (arrows). Distinctive features between afferent fibers cannot be made at this magnification. The granule cell groups (GC), a dark Purkinje cell (PC) and capillaries are also distinguished. Araldite embedded material. Toluidine blue staining.

Fig. 2. Cryoprotected freeze-fractured rat cerebellum. SEM micrograph of the white matter (WM) of the cerebellar folia, displaying the extrinsic fibers (arrows) which follow a radial course from the center of the white matter toward the granular layer (GL).

Fig. 3. Cryoprotected freeze-fractured rat cerebellum. SEM micrograph at higher magnification of thick caliber-mossy fiber (arrows) and thin caliber climbing fibers (arrowhead). Interfasicular oligodendroglial cells and fine filamentous processes are distinguished among them.

Fig. 4. Photomicrograph of teleost fish (Arius spixii) cerebellar cortex showing the granular (GL), Purkinje cell (PL) and molecular layers (ML). Araldite embedded material. Toluidine blue staining.

Fig. 5. Photomicrograph of teleost fish (Arius spixii) cerebellar cortex illustrating the fibrous stratum (FS) located between the Purkinje (PL) and granular layers (GL). Araldite embedded material. Toluidine blue staining.

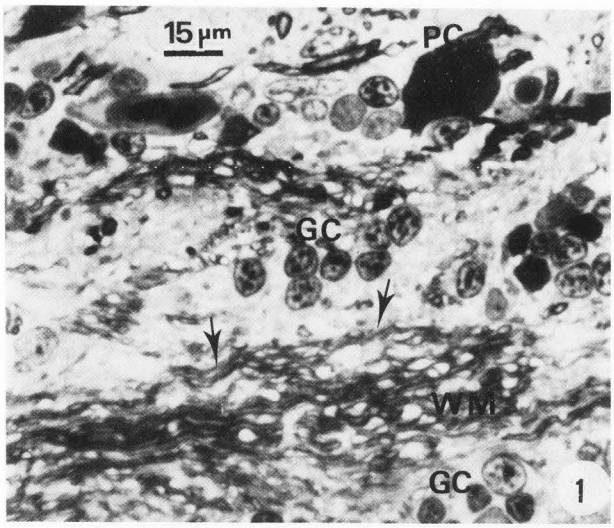
15 µm
PC
GC
WM
GC
1

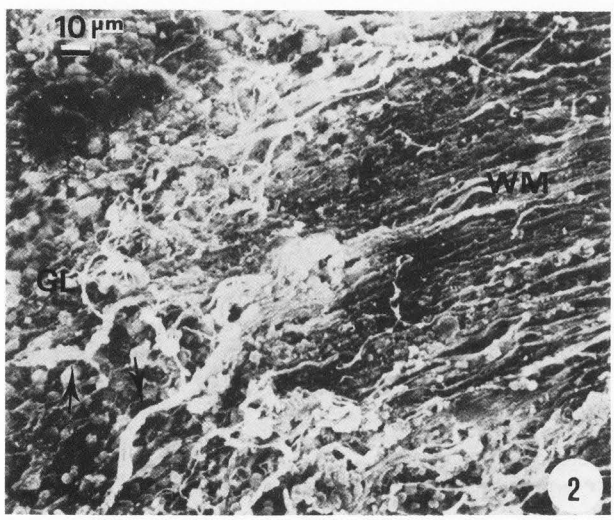
10 µm
WM
GL
2

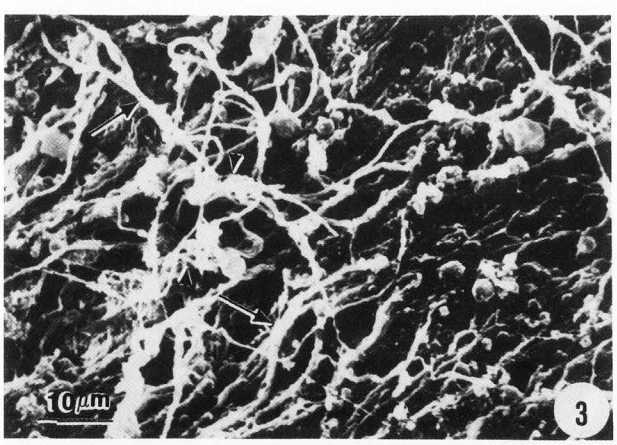
10 µm
3

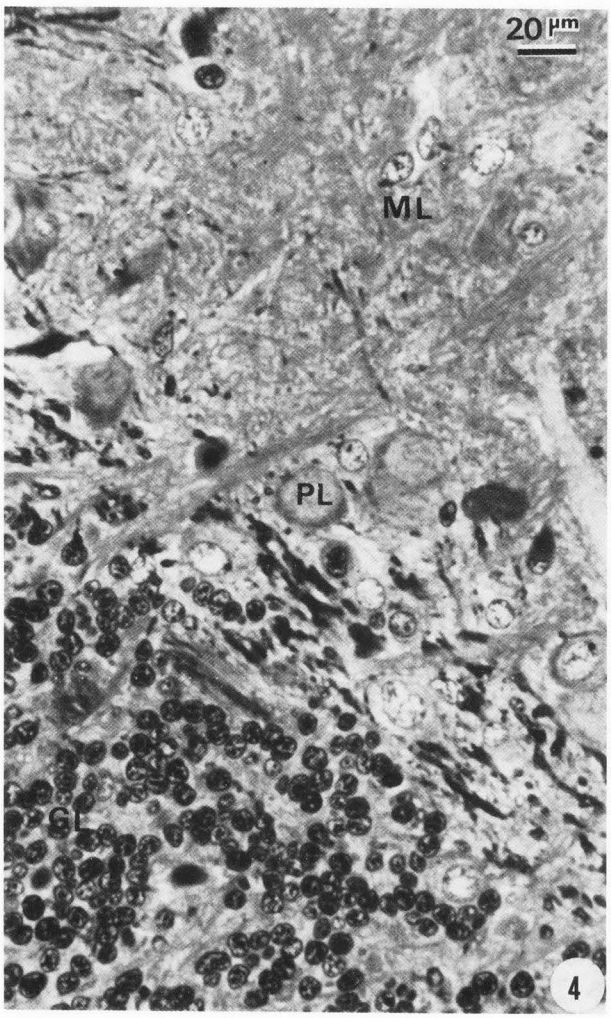
20 µm
ML
PL
GL
4

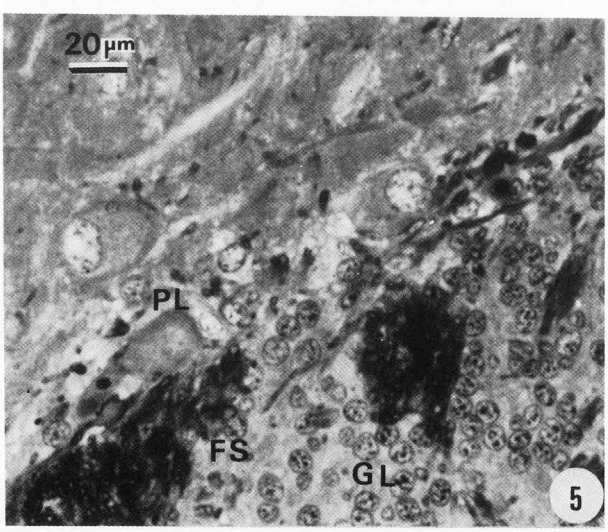
20 µm
PL
FS
GL
5

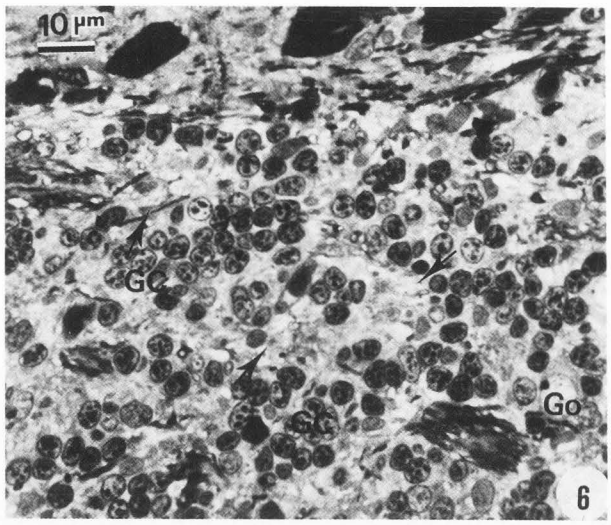
10 µm
GC
Go
6

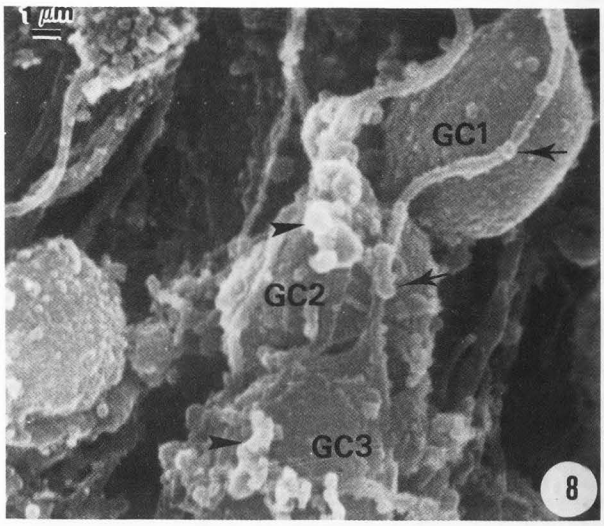
1 µm
GC1
GC2
GC3
8

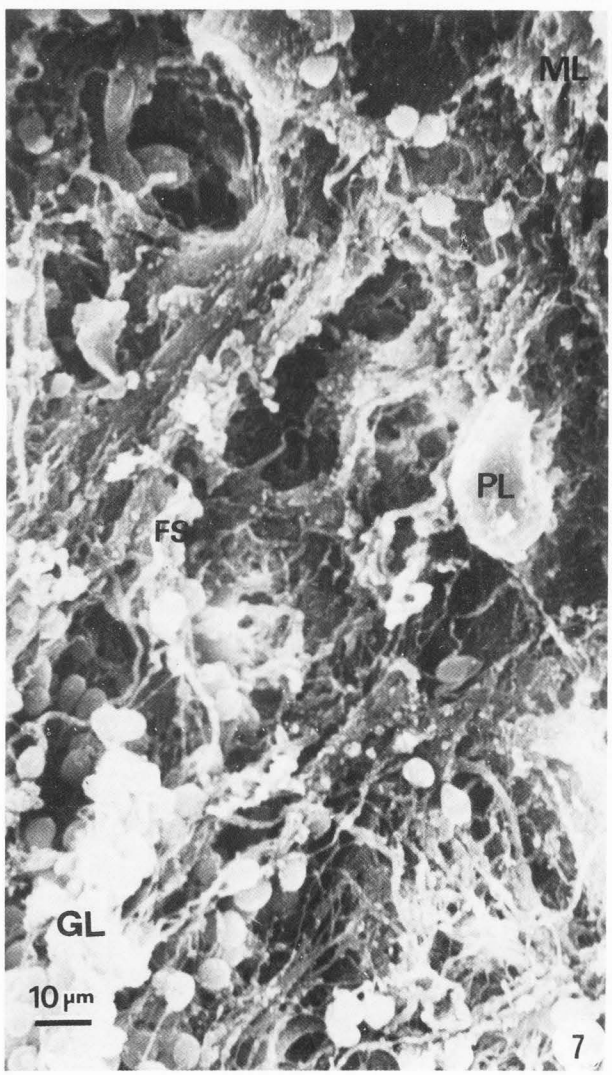
ML
PL
FS
GL
10 µm
7

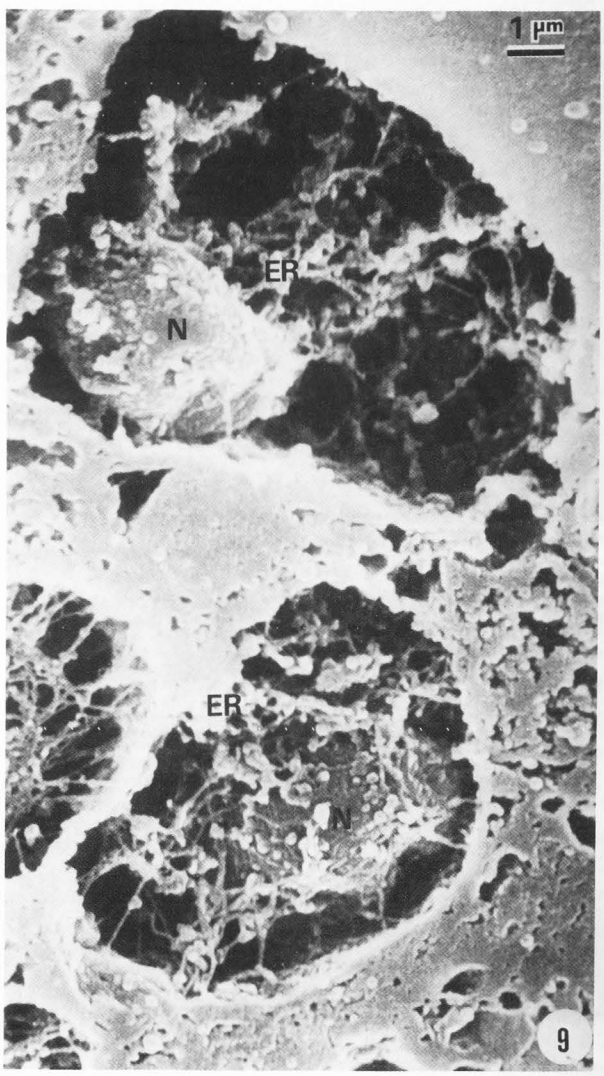
1 µm
ER
N
ER
N
9

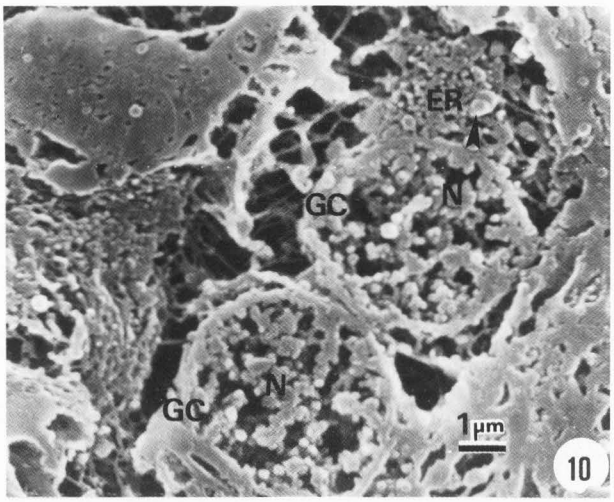

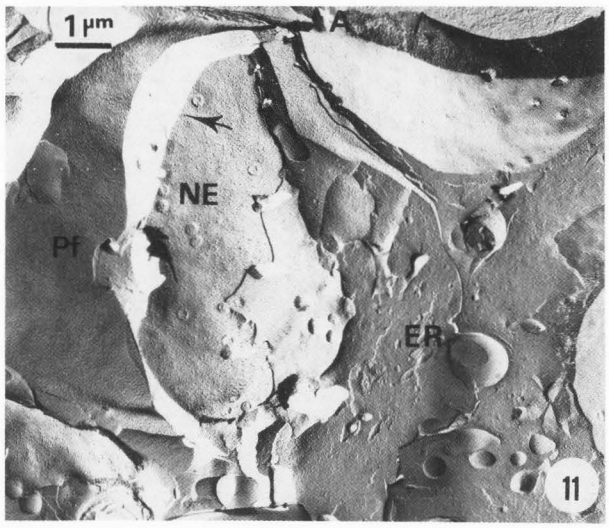

Fig. 6. Photomicrograph of teleost fish (Arius spixii) cerebellar cortex, exhibiting the granule cell groups (GC), separated by clear spaces corresponding to the glomerular regions (arrows). A Golgi cell (Go) is also seen. Araldite embedded material. Toluidine blue staining.
Fig. 7. SEM micrograph of teleost fish (Arius spixii) processed by the slicing technique. The granular layer (GL), fibrous stratum (FS), Purkinje (PL) and molecular layers (ML) are clearly visualized.
Fig. 8. SEM micrograph of teleost fish (Arius spixii) processed by the slicing technique. Three spherical granule cell bodies are distinguished (GC1, GC2, GC3). The ascending granule cell axon (arrows) shows a filiform shape. The granule cell dendrites (arrowheads) appear as short, twisted processes.
Fig. 9. SEM micrograph of Salmo trout cerebellar cortex processed by the freeze-fracture method showing the fractured granule cells. The outer surface of the nucleus (N) and endoplasmic reticulum (ER) are seen. The washing out process of cytoplasmic soluble proteins induces a caveolar appearance of the cytoplasm.
Fig. 10. SEM micrograph of Salmo trout cerebellar cortex processed by the freeze-fracture method. Two fractured granule cells (GC) exhibit the nuclear heterochromatin anastomotic bands (N) and the spatial organization of endoplasmic reticulum (ER), extended between the nucleus and the plasma membrane. The arrowhead indicates the Golgi complex.
Fig. 11. Freeze-etching replica of mouse cerebellar granular layer showing a fractured granule cell. The cleavage plane permitted us to visualize the P face of the plasma membrane (Pf), the width of the perikaryal cytoplasm (arrow), the fractured nuclear envelope (NE) and the cytoplasmic fracture face with scarce endoplasmic reticulum profiles (ER).

by the dendritic processes. The mossy rosettes were not really visualized since they were encapsulated by the dendritic digits. The mossy fiber emerging from the clew could be traced for a short distance to penetrate again into a neighboring glomerulus (Fig. 14). This observation confirms the "en passant" type of mossy fiber synaptic contacts. We have counted up to 18 granule cells surrounding a mossy fiber rosette and distinguished as many as 17 granule dendrites converging into a single mossy fiber (Fig. 15). Remnants of neuroglial cytoplasm appeared partially covering the mossy glomerular regions which in turn, acquire a rugged appearance.

The parent mossy fibers and their branches were identified in SEM freeze-fracture fish specimens by their typical rosette formations (Fig. 16). At the level of the fractured glomerulus, the mossy fiber appeared as a thick axon showing at regular intervals, smooth surface fusiform or ellipsoidal enlargements which make contact with several triangular granule cell dendritic digits. The foci of expansion of the mossy fiber could be well and easily correlated with those observed in Golgi impregnated material (Castejón, 1981). Two complementary techniques, conventional TEM and freeze-etching have shed information on the internal structure of mossy rosettes of rodent cerebellar cortex. At the TEM level, the mossy rosettes of mouse cerebellar cortex contained numerous clear, spheroidal vesicles and mitochondria (Fig. 17).The mossy endings establish Gray's type I or asymmetric synaptic contacts with the granule cell dendritic claw (Gray, 1961; Castejón, 1971).

In freeze-etching replicas, the cytoplasmic fracture face of mossy rosettes (Fig.18) exhibited numerous spheroidal synaptic vesicles and mitochondria randomly dispersed throughout the homogeneous, smooth surface matrix of the terminal. Several granule cell dendritic processes appeared surrounding and invaginating the mossy rosette surface (Fig. 19). The P face of both structures displayed a characteristically increased number of intramembrane particles. Toward the glomerular periphery, the smooth cytoplasmic fracture face of neuroglial cytoplasm was also distinguished.

Climbing fiber glomerulus. The climbing fibers appeared in teleost fish cerebellar cortex processed by the slicing technique for SEM, as large thick axons crossing the granule cell layer (Fig. 20). Two different types of collaterals, as previously described by Palay and Chan-Palay (1974) in camera lucida observations, were seen emerging from the climbing fiber during its course through

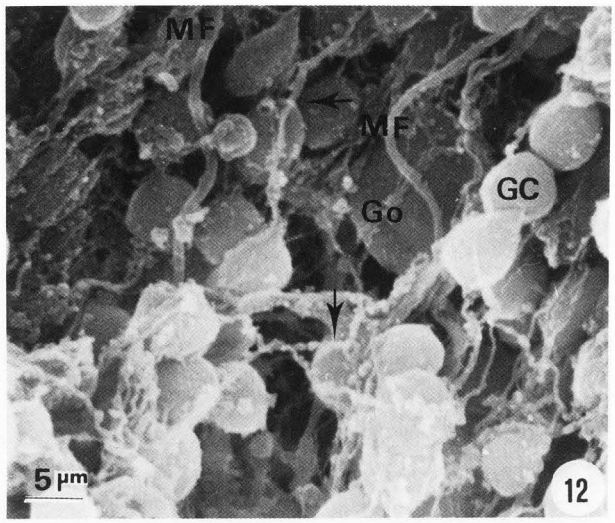

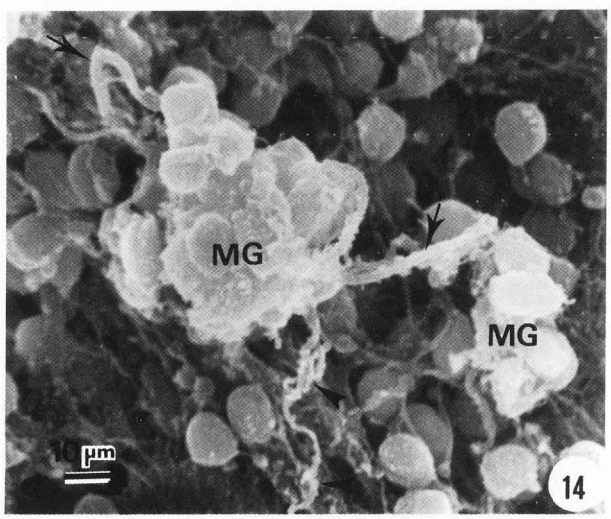

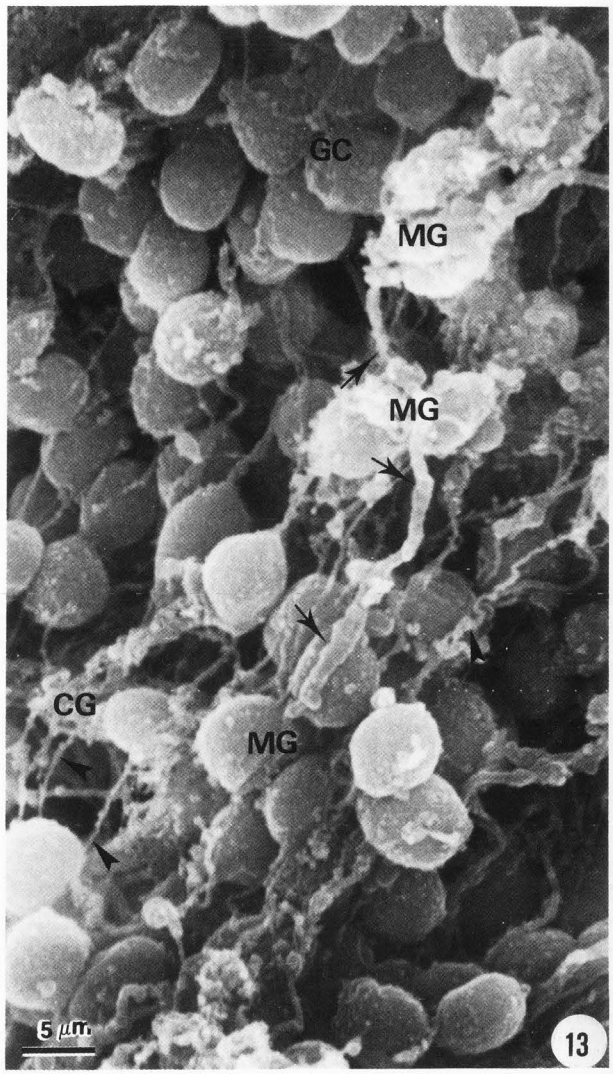

Fig. 12. SEM micrograph of teleost fish (Arius spixii) cerebellar granular layer processed by the slicing technique. Two thick mossy fibers (MF) are observed. Fine tendril collaterals of climbing fibers (arrows) appear between the mossy fibers. A Golgi cell soma (Go) is also seen surrounded by granule cells (GC).
Fig. 13. SEM micrograph of teleost fish (Arius spixii) cerebellar granular layer processed by the slicing technique. A thick, en passant, mossy fiber (arrows) appears participating in the formation of three successive mossy glomeruli (MG). The fine tendril collaterals of climbing fibers (arrowheads) are also seen among the granule cells (GC) forming the climbing glomeruli (CG).
Fig. 14. SEM micrograph of teleost fish (Arius spixii) cerebellar granular layer processed by the slicing technique. A fine beaded process, presumably belonging to a Golgi cell axon (arrowhead) is observed contributing to the formation of mossy glomerulus (MG). The mossy fiber (arrows) is observed entering and leaving the granule cell groups.
Fig. 15. SEM micrograph of teleost fish (Arius spixii) cerebellar granular layer processed by the slicing technique showing an en face view of the mossy glomerular region. Up to 14 granule cells (GC) appear sending their dendrites toward the central mossy fiber rosette (MR).
Fig. 16. SEM micrograph of teleost fish (Arius spixii) processed by the freeze-fracture method revealing a transversal view of mossy glomerular region. The mossy fiber (MF) appears surrounded by the granule cell dendrites (arrows) during its course through various granule cells (GC).
Fig. 17. TEM micrograph of mouse cerebellar cortex processed by glutaraldehyde-osmium tetroxide immersion technique showing the mossy glomerulus. The mossy fiber rosette (MR), containing numerous clear spheroidal synaptic vesicles (SV) and mitochondria (M), appears surrounded by granule cell dendrite profiles (Gd). The arrows indicate asymmetric or Gray's type I synaptic contacts.
Fig. 18. Freeze-etching replica of mouse cerebellar cortex showing the three-dimensional view of a fractured mossy fiber glomerulus. The central mossy fiber rosette (MR) contains spheroidal synaptic vesicles (SV), and mitochondria (M). The arrow indicates the P face of mossy fiber presynaptic membrane showing the distribution of intramembrane particles. The fractured profiles of granule cell dendrites (Gd) are seen in relief indenting the mossy rosette surface. The cytoplasmic fracture face of neuroglial cells (NC) are observed at the periphery of the mossy glomerulus.

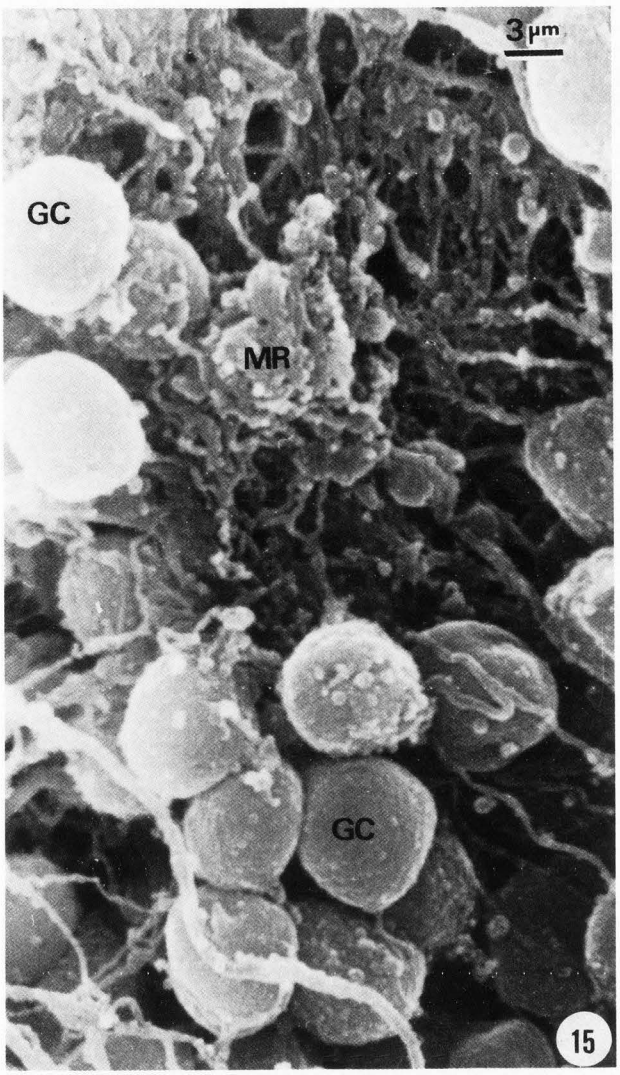
3 µm
GC
MR
GC
15

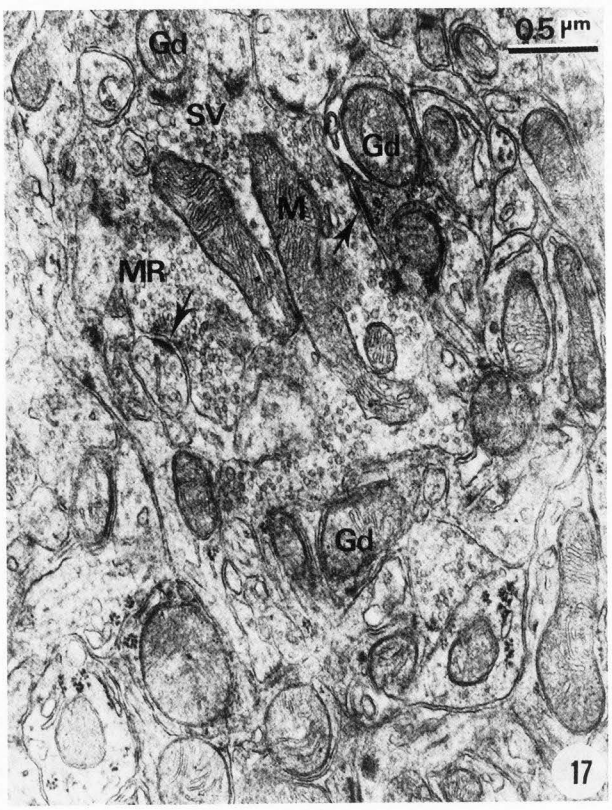
0.5 µm
Gd
SV
Gd
M
MR
Gd
17

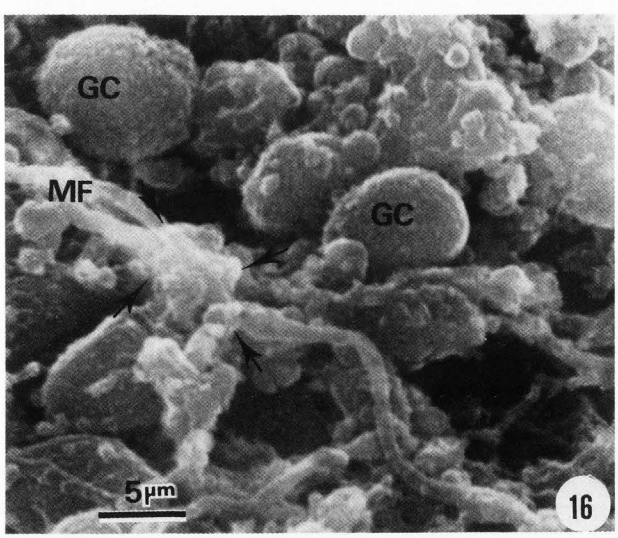
GC
MF
GC
5µm
16

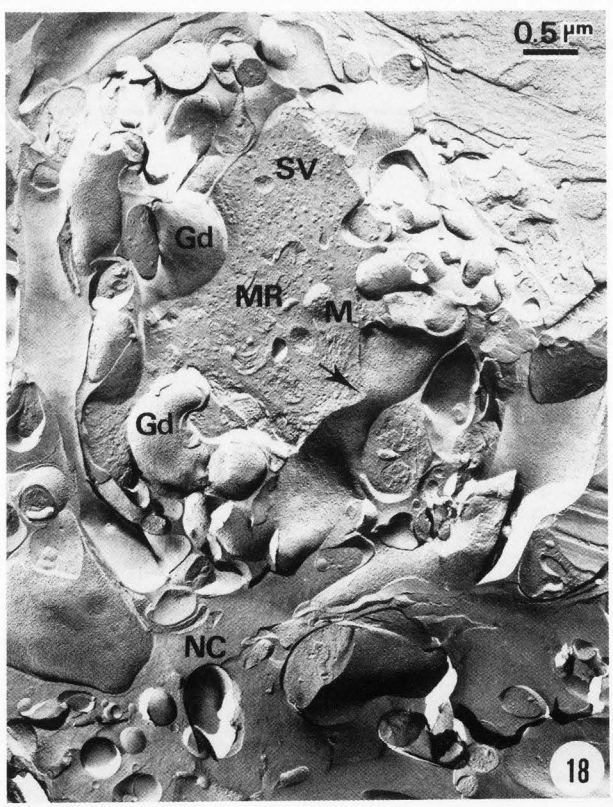
0.5 µm
SV
Gd
MR
M
Gd
NC
18

this layer. The first type, the fine tendril collaterals, characterized by varicosities or globular enlargements connected by a fine thread, closely resembling the Golgi cell axonal ramifications, and the second type or thick collaterals (Palay's glomerular collaterals), which fairly maintain the same caliber as the parent stem and end in a truncated spray or large efflorescence. These latter collaterals could be seen participating in the formation of glomeruli. The climbing fiber glomeruli (Fig. 21) appeared as thin elongated structures, in which the glomerular collaterals were surrounded by the granule cell dendritic digits. They could be clearly differentiated from the mossy fiber glomeruli, since the latter ones were larger and round or polygonal, due to the presence of the mossy rosette core. As previously described (Castejón and Caraballo, 1980a), the Golgi cell axonal plexuses have been also seen participating in the formation of these glomeruli. The neuroglial envelope was apparently absent from the climbing glomeruli, since vestiges of neuroglial cytoplasm, as seen in the mossy fiber glomeruli, were not clearly distinguished.

Golgi cells. These cells, examined in teleost fish and human cerebelli by Golgi light microscope technique and SEM, are macroneurons located among the granule cell groups (Fig.12) and characterized by their large size, horizontal and ascending dendrites and typical highly branched axonal plexuses (Figs. 22 and 23). Ethanol-cryofracturing technique for SEM has allowed us to study individual Golgi cells and their processes (Castejón and Caraballo, 1980b). In human cerebellar cortex, it was possible to observe that the horizontal or descending dendrites remain in the granular layer and can be followed toward the neighboring glomeruli. The ascending dendrites enter the Purkinje cell layer on their way to the molecular layer. In teleost fish cerebellar cortex, it has been impossible thus far, to characterize by SEM, the ascending and horizontal dendrites due to the superposed adjacent granule cells. The Golgi cell axon (Fig.23) appears highly ramified and each axonal branch has a beaded shape showing successive constrictions and dilations. This appearance facilitates its identification in the granular layer, especially at the periphery of the mossy glomerular region. The axonal endings synapse with granule cell dendrites (Fig. 24) which ramify extensively in the granular layer, giving the impression of a network or cobweb joining the granule cell clusters and glomerular islets. As previously mentioned, the Golgi axons participate in the formation of mossy and climbing glomeruli (Fig.14). The differentiation between Golgi axonal ramifications and tendril collaterals of climbing fibers was difficult because of the similar topographic distribution of both axonic processes in certain areas, especially in those SEM electron micrographs where the parent stems were not visualized. The beaded shape of these ramified types adds a source of uncertainty.

Purkinje cell layer. At this layer, the Golgi light microscope preparations of mouse and fish cerebellum showed the Purkinje cells with their typical pear or flask shaped cell soma, and at the molecular layer, the profusely elaborated dendritic tree, characterized by a primary dendritic trunk, and secondary and tertiary branches (Fig. 25). Basket cell axons appeared transversally running over the Purkinje cell and impinging upon the soma surface contributing to the formation of the pericellular basket. A similar and improved view could be obtained with the ethanol-cryofracturing technique for SEM applied to human cerebellum (Fig. 26). In these preparations, the Purkinje cells (Fig. 27) exhibited a rough surface, the attached basket cell axosomatic synaptic endings and debris of neuroglial processes.

In transmission electron micrographs, the mouse Purkinje cell surface appeared ensheathed by Bergmann glial cells, axosomatic contacts of basket cell axons and axospinodendritic contacts of climbing fibers (Fig. 28). The ethanol-cryofracturing technique induced an artifactual removal of the satellite Bergmann glial cells, allowing the exploration of the incoming processes forming the pericellular basket. The descending collaterals of basket cell axons appeared as rounded or digitiform processes surrounding the perikaryon of the Purkinje cell and forming short or extensive terminals or "en passant" axosomatic junctions. These descending collaterals continue beyond the cell body forming the pinceaux which surround the initial segment of the Purkinje cell axon. In addition, climbing fiber stems and their tendril collaterals could be observed passing through the pinceaux on their way to the molecular layer (Castejón and Valero, 1980).

In comparison with human cerebellum, with the

Fig. 19. Freeze-etching replica of mouse cerebellar cortex illustrating the three-dimensional view of mossy glomerulus peripheral region. The mossy rosette (MR) shows the continuity with the mossy fiber (arrow) suggesting its "en passant" nature. The complex interdigitation between granule cell dendrites (Gd) and neuroglial cytoplasm (NC) is appreciated.

Fig. 20. SEM micrograph of teleost fish (Arius spixii) cerebellar granular layer processed by the slicing technique. A climbing fiber glomerular collateral (CF1) and a granule cell (GC) appear contributing to the formation of a climbing fiber glomerulus (CG). Another climbing fiber (CF2) ascends to the Purkinje cell layer.

Fig. 21. SEM micrograph of teleost fish (Arius spixii) cerebellar granular layer processed by the slicing technique. A glomerular collateral of a climbing fiber (CF) is observed bifurcating (arrows) and forming two thin, elongated climbing fiber glomeruli (CG1, CG2).

Fig. 22. Photomicrograph of teleost fish Golgi stained cerebellar cortex. The Golgi cell (Go) exhibits the beaded axonal ramification extended in the granular layer (arrowheads). An ascending dendrite (arrow) is also seen.

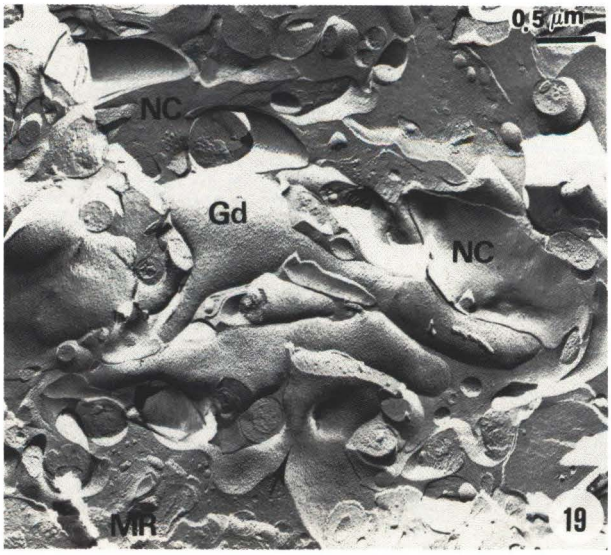
0.5 µm
NC
Gd
NC
MR
19

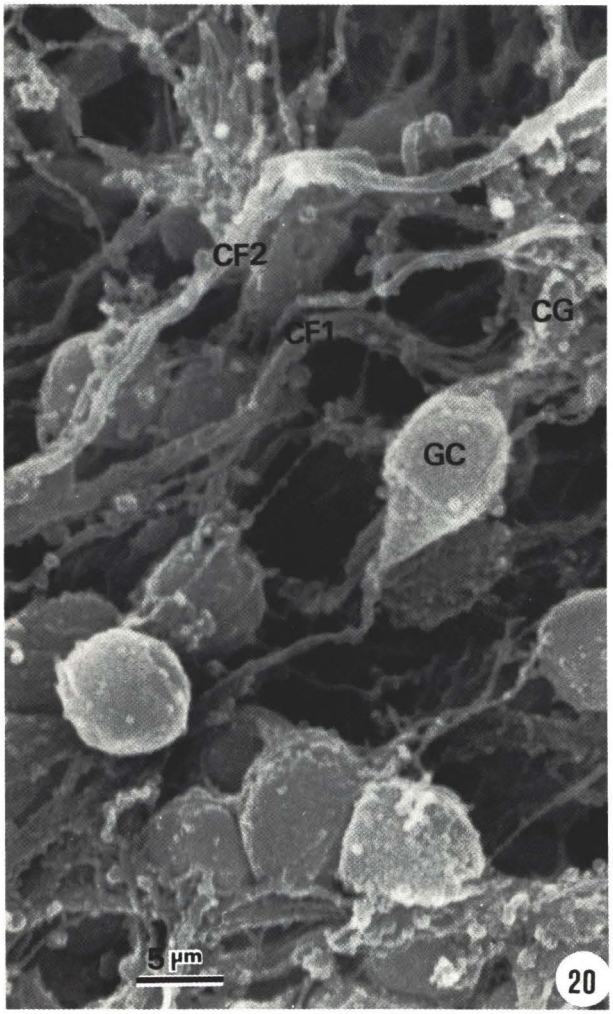
CF2
CF1
CG
GC
5 µm
20

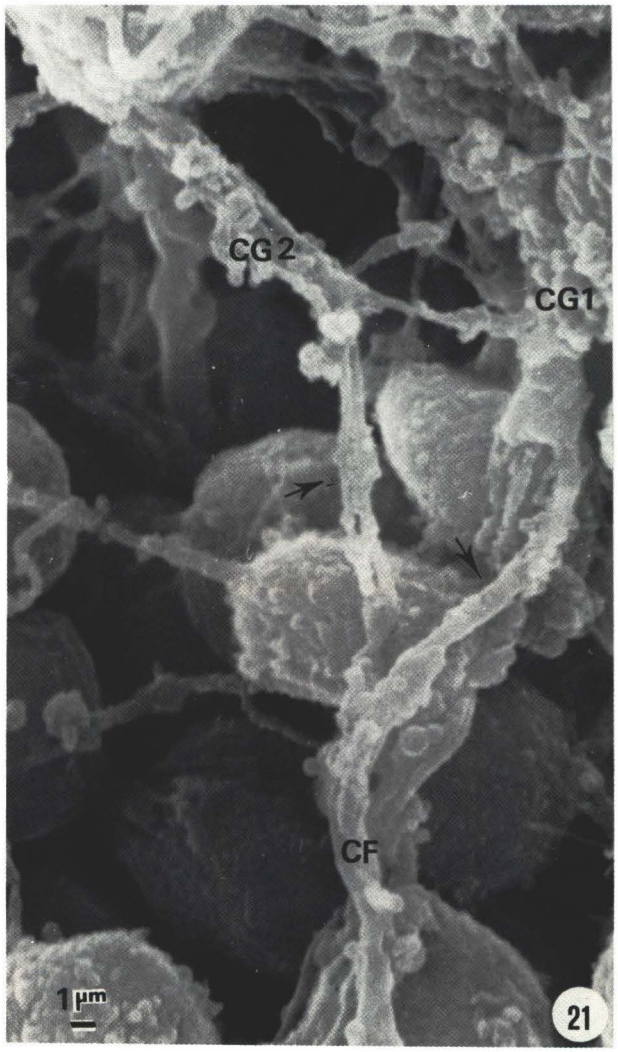
CG 2
CG1
CF
1 µm
21

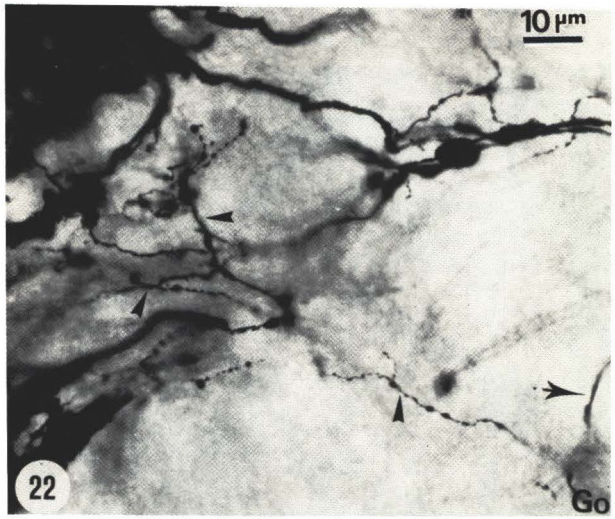
10 µm
22
Go

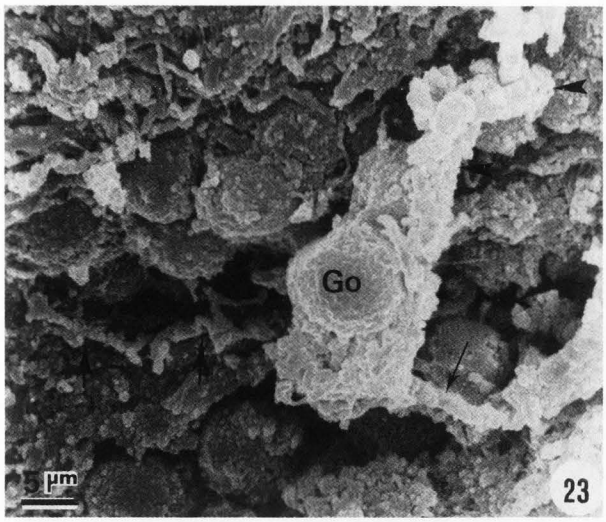
Go
5 µm
23

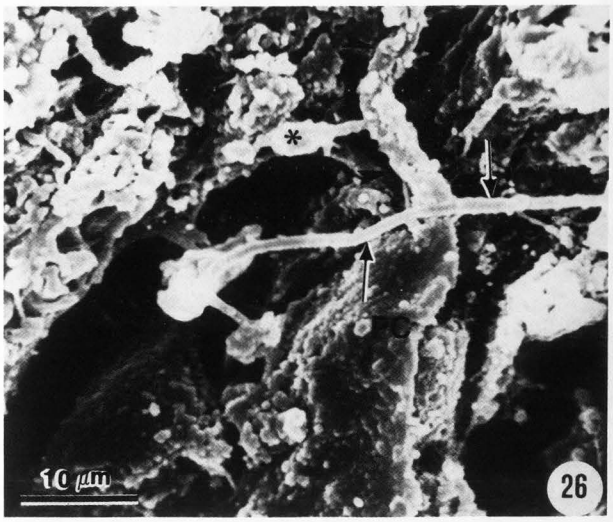
*
10 µm
26

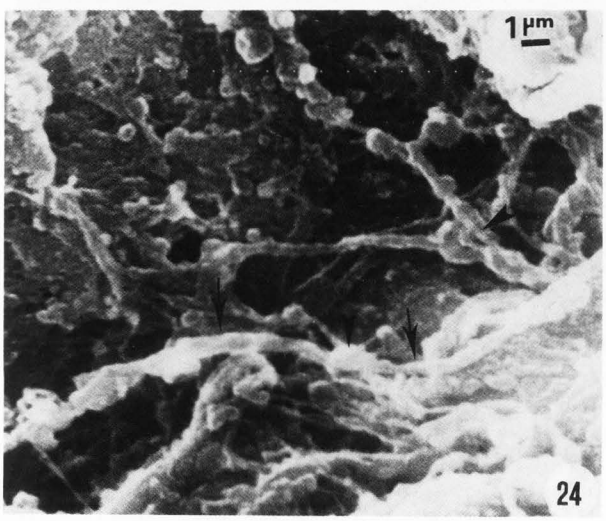
1 µm
24

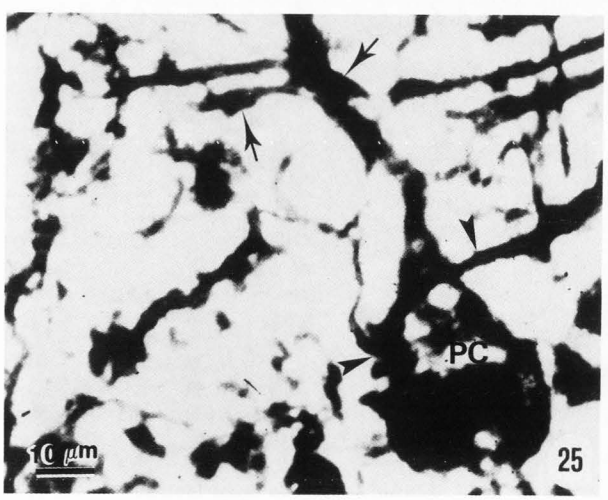
PC
10 µm
25

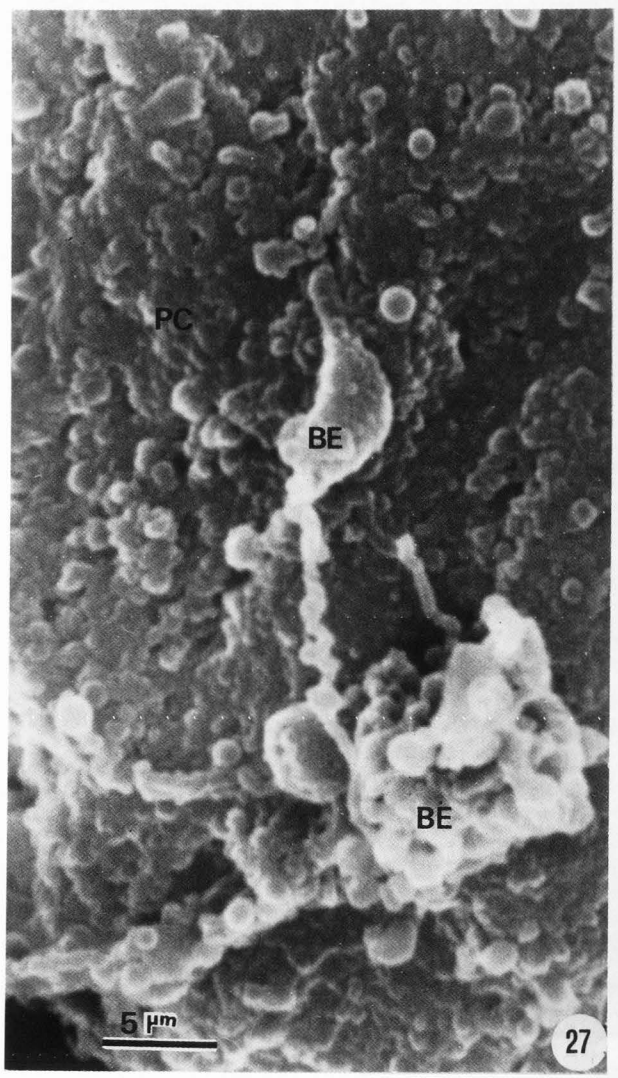
PC
BE
BE
5 µm
27

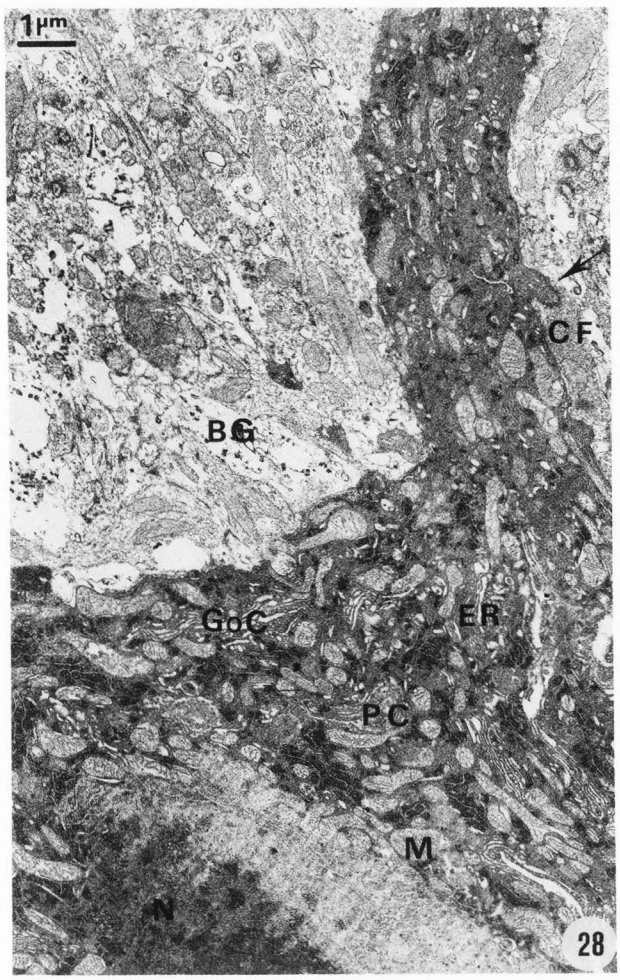

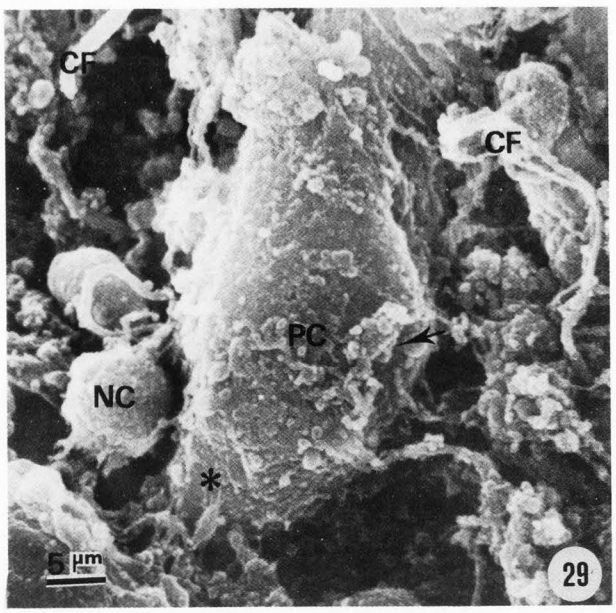

SEM slicing technique, a better preservation of teleost fish Purkinje cell was obtained. The shape, outer surface and topographical relationship of Purkinje cell soma with ascending climbing fibers and neighboring basket cells (Fig. 29) were clearly visualized. The cleavage plane was again undoubtedly produced at the level of satellite Bergmann glial cells.

Close examination of freeze-etching replicas permitted a three-dimensional view of cytoplasmic and nuclear fracture faces of Purkinje cell soma (Fig. 30). This image could be easily correlated with the TEM electron micrograph illustrated in

Fig. 23. SEM micrograph of human cerebellar cortex processed by the ethanol-cryofracturing technique. A Golgi cell (Go) is observed exhibiting the beaded axonal plexus (thick arrows) and a horizontal dendrite (thin arrow) remaining in the granular layer and an ascending dendrite (arrowheads) directed toward the molecular layer.

Fig. 24. SEM micrograph of teleost fish (Arius spixii) processed by the freeze-fracture method. Fine beaded axonal ramifications of Golgi cell (arrows) are observed synapsing with granule cell dendritic digits (arrowheads).

Fig. 25. Photomicrograph of mouse cerebellar cortex irregularly stained by the Golgi method. The Purkinje cell (PC) soma and the dendritic arborization (arrows) are clearly distinguished. A basket cell axon (arrowheads) appears running transversally over the somatic surface contributing to the formation of the pericellular basket.

Fig. 26. SEM fractograph of human cerebellar cortex processed by the ethanol-cryofracturing technique. The shrunken Purkinje cell (PC) soma shows the emergence of the primary dendritic trunk (arrowheads). A climbing fiber (asterisk) is seen approaching to the primary trunk. A transversally running basket cell axon (arrows) participates in the formation of the Purkinje pericellular nest. The Bergmann glial cell has been detached by the cryofracturing process at the dark spaces surrounding the Purkinje cell.

Fig. 27. SEM fractograph of human cerebellar cortex processed by the ethanol-cryofracturing technique. Axosomatic endings of basket cell axons (BE) are observed attached to the exposed Purkinje cell surface (PC).

Fig. 28. TEM of mouse cerebellar cortex showing a dark Purkinje cell (PC) and its primary dendritic trunk. The nucleus (N), endoplasmic reticulum (ER), mitochondria (M) and Golgi complex (GoC) are observed. The electron lucent cytoplasm of Bergmann glial cells (BG) appears partially covering the somatic surface. A climbing fiber ending (CF) is seen synapsing with a spine at the level of the primary dendritic trunk (arrow).

Fig. 29. SEM micrograph of teleost fish (Arius spixii) processed by the slicing technique. The pyriform Purkinje cell body (PC) appears surrounded by axosomatic endings of basket cell (arrow) and a neuroglial cell (NC). Climbing fibers (CF) are distinguished. The surface of the axon hillock region of the Purkinje cell (asterisk) is also seen at the lower pole of cell soma.

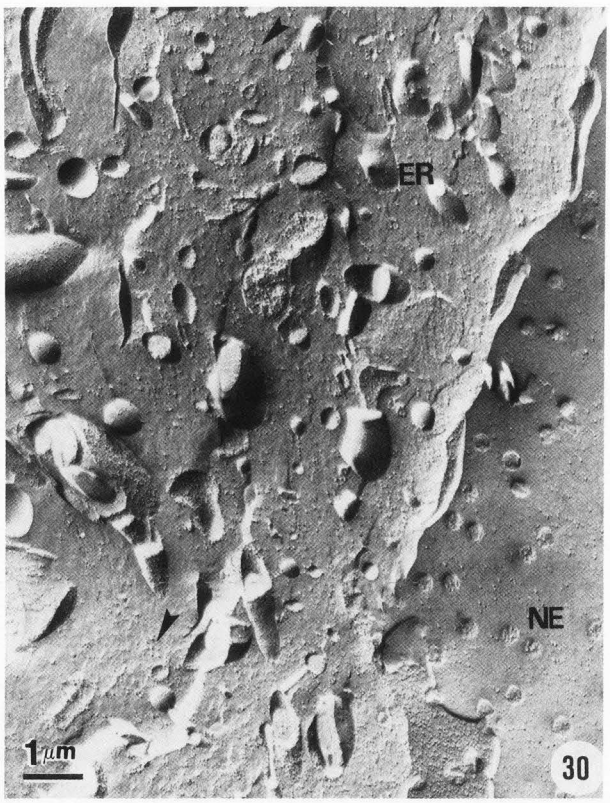

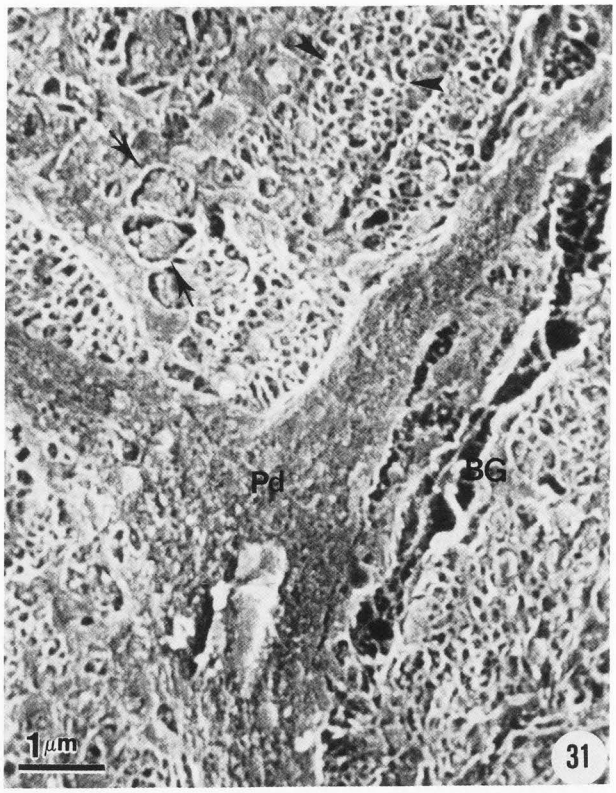

Fig. 28. A complete description of the fine structure of Purkinje cell soma by means of transmission electron microscopy has been given by Palay and Chan-Palay (1974).

As illustrated in human cerebellum (Fig. 26), the primary dendritic trunk of Purkinje cells could be observed projecting vertically and devoid of the neighboring neuropil. The surface of the trunk showed small and fine attached processes, presumably corresponding to remaining portions of neuroglial cytoplasm and synaptic endings of climbing fibers and basket cell axons.

Molecular layer. At this layer, the Purkinje dendritic arborization, parallel and climbing fibers, stellate neurons, neuroglial cells and capillaries were recognized.

With the SEM freeze-fracture method a true appreciation of the three-dimensional configuration of fractured Salmo trout Purkinje dendritic arborization was obtained. Secondary, tertiary and successive dendritic branches were observed ascending or curling downwards in the molecular layer (Fig. 31). The cross sections of passing parallel fibers and the synaptic varicosities of these fibers were seen forming the immediate neighboring

Fig. 30. Freeze-etching replica of mouse cerebellar cortex displaying the three-dimensional relief of fractured endoplasmic reticulum (ER), cell organelles and nuclear envelope (NE) of Purkinje cell soma. Free ribosomes and polyribosomes are seen embedded on the cytoplasmic fracture face (arrowheads).
Fig. 31. SEM micrograph of Salmo trout cerebellar cortex processed by the freeze-fracture technique. The fractured primary trunk and secondary Purkinje dendrites (Pd) are ensheathed by the Bergmann glial cell cytoplasm (BG). The cross cut synaptic endings (arrows) and non-synaptic segments of parallel fibers (arrowheads) are observed in the neighboring neuropil.
Fig. 32. SEM micrograph of human cerebellar molecular layer processed by the ethanol-cryofracturing technique. A parallel fiber (arrows) is observed passing through successive Purkinje dendritic branches making "en passant" synapses (arrowheads) with Purkinje dendritic spines (Ps).
Fig. 33. Freeze-etching replica of mouse cerebellar molecular layer fractured in the sagittal plane. Two longitudinally fractured Purkinje dendrites (Pd1, Pd2) appear separated by cross cut parallel fiber bundles (PF). A climbing fiber ending (CF) and a capillary (C) are also seen.
Fig. 34. Freeze-etching replica of mouse cerebellar molecular layer fractured in the transversal plane. The longitudinal profile of a parallel fiber (PF) is seen covered by the Bergmann glial cell cytoplasm (BG). An opening through the synaptic varicosity allows one to visualize the spheroidal synaptic vesicles (arrow). The P face (Pf) and E face (Ef) of neighboring endings of Purkinje spines are also distinguished.
Fig. 35. Freeze-etching replica of mouse cerebellar molecular layer. The fractured Purkinje branchlet (Pd) exhibits the E face of three Purkinje spines (Ps). The three-dimensional morphology of the spines is illustrated in relief over the smooth cytoplasmic fracture face of Bergmann glial cell (BG). In the upper part of the figure the parallel fibers (PF) can be seen.

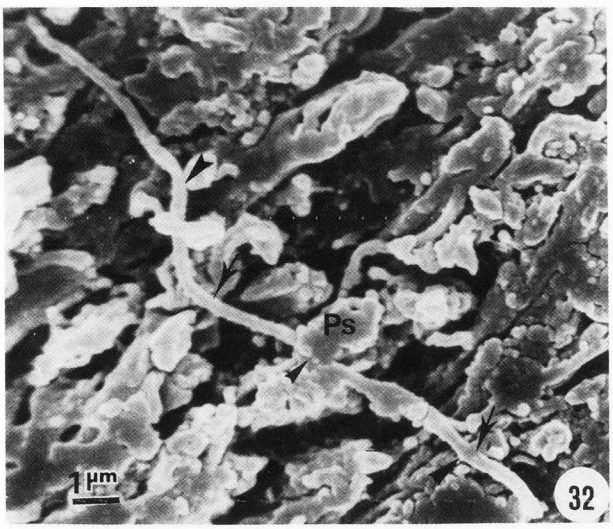
Ps
1 µm
32

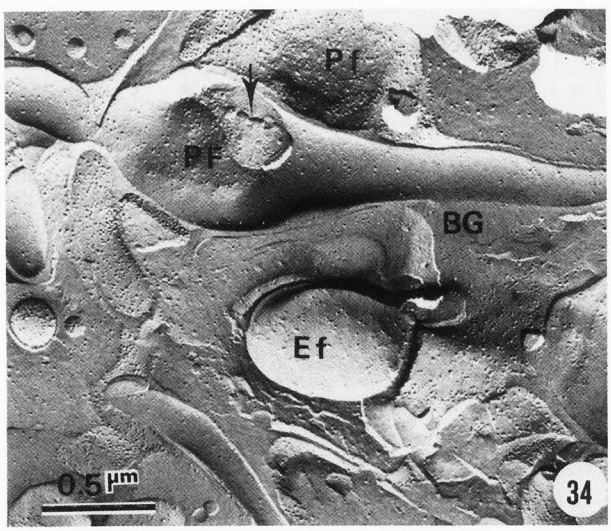
Pf
PF
BG
Ef
0.5 µm
34

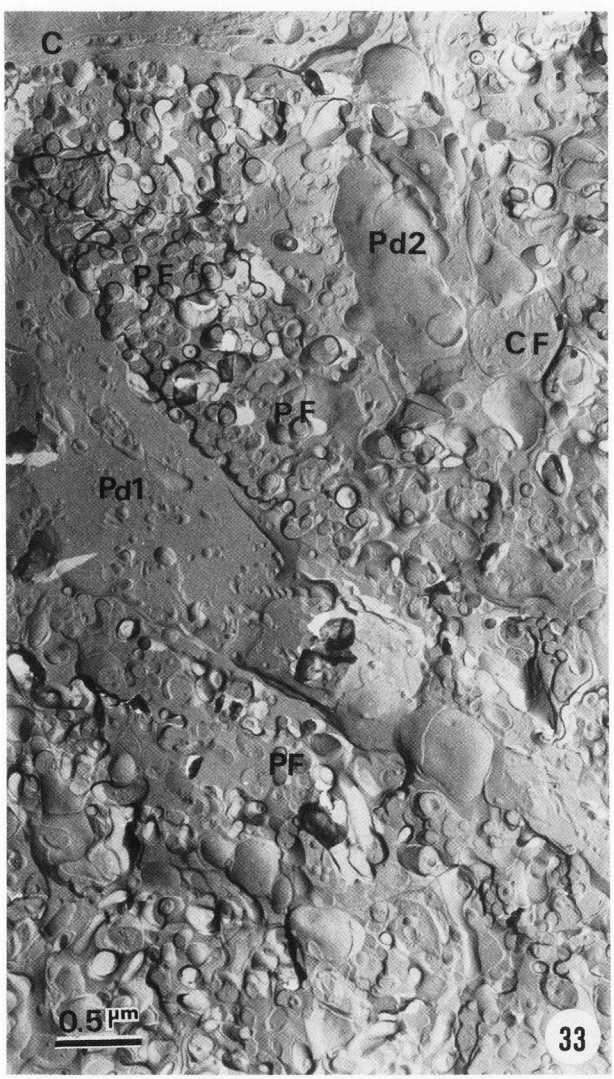
C
Pd2
PF
CF
PF
Pd1
PF
0.5 µm
33

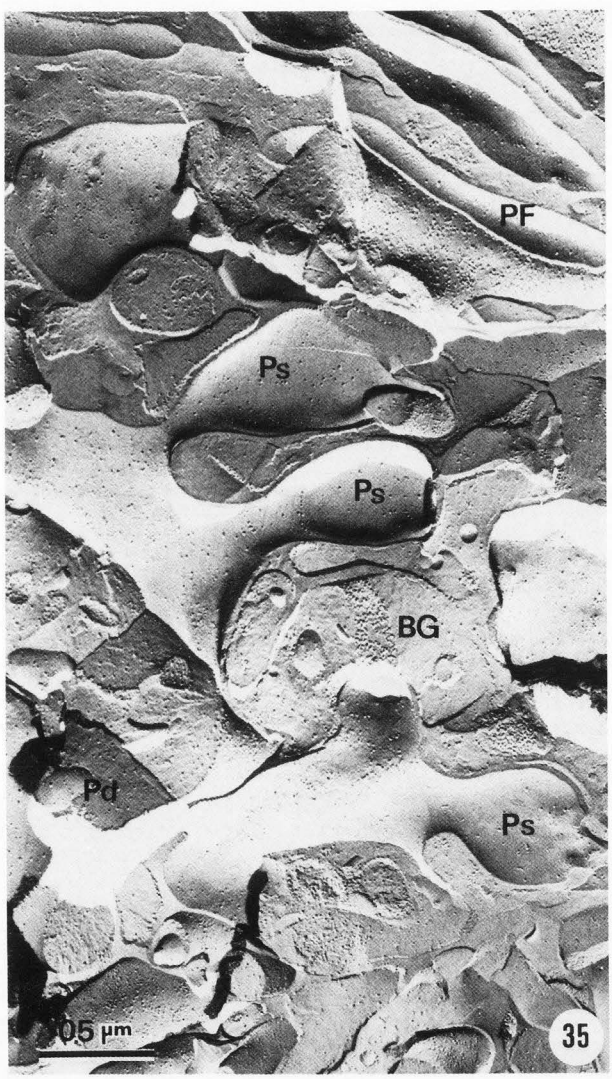
PF
Ps
Ps
BG
Pd
Ps
0.5 µm
35

neuropil. In spite of the low SEM resolution, the three-dimensional image of spheroidal synaptic vesicles was observed within the parallel "en passant" synaptic endings. With the SEM freeze-fracture technique, preservation of the Bergmann glial cytoplasm was achieved, presumably due to the rapid freezing by Freon 22. As previously mentioned, these neuroglial cells were not seen with the ethanol-cryofracturing technique, in which liquid nitrogen (medium freezing rate) was used.

Parallel fiber-Purkinje dendrite synaptic relationship. With ethanol-cryofracturing technique, the "en passant" synaptic relationship between Purkinje dendrites and parallel fibers was recognized in human cerebellum (Fig. 32). The parallel fiber appeared as a thin filiform structure passing through the successive Purkinje dendritic branchlets.

A deeper and more detailed information on the three-dimensional arrangement of the parallel-Purkinje spine synapses was obtained through the study of freeze-etching replicas of mouse cerebellar molecular layer. After the T bifurcation in this layer, the granule cell axons or parallel fibers could be identified because they run perpendicularly orientated to the Purkinje dendritic arborization. The cross section of the synaptic enlargements and the non-synaptic segments of the parallel fibers could be seen in the immediate neighborhood of the primary, secondary and tertiary Purkinje dendrites (Fig. 33). In sections passing through the longitudinal axis of the cerebellar folium, the parallel fibers were seen in relief, showing the synaptic varicosities related to the Purkinje dendritic spines and the non-synaptic segments covered by the Bergmann glial cell cytoplasm. The fractured "en passant" synaptic endings of parallel fibers appeared as large round profiles which contained clusters of spheroidal synaptic vesicles (Fig. 34).

Fig. 35 illustrates a fractured Purkinje dendritic branchlet exhibiting the three-dimensional morphology of Purkinje spines E face. They exhibit a short neck, an elliptical body and a round end, partially ensheathed by the Bergmann glial cell cytoplasm. At the TEM level the Purkinje dendritic spines were observed making Gray's type I synaptic contacts or asymmetric synapses with the "en passant" varicosities of parallel fibers (Fig. 36). In freeze etching preparations the fractured presynaptic varicosities of parallel fibers, containing spheroidal synaptic vesicles (Fig. 37) appeared attached to the bulbous round end of the spine, making invaginated spine synapses.

With the freeze-fracture method for SEM, in spite of the low SEM resolution, a three-dimensional view of Salmo trout parallel fiber varicosities was achieved (Fig. 38). The fractured endings showed closely packed spheroidal vesicles clustered by an amorphous substance. In freeze-etching replicas of mouse cerebellar cortex, an aggregation of intramembrane particles was observed at the P face of mouse parallel presynaptic membrane and at the E face of Purkinje postsynaptic membrane (Fig. 39). The cytoplasmic fracture face of Bergmann glial cells appeared encapsulating the spine synapses. The parallel fiber varicosity appeared surrounding the Purkinje dendritic spine making invaginated spine synapses. This arrangement could be easily correlated with the TEM appearance of cross sectioned parallel fiber-Purkinje spine synapses (Fig. 40). With the SEM freeze-fracture method, the non-synaptic segments of teleost fish (Arius spixii) parallel fibers were observed as a compact bundle of cylindrical axons separated by neuroglial cytoplasm (Fig. 41). In mouse freeze-etching replicas, the P face of parallel fiber membrane was disclosed showing numerous randomly dispersed intramembrane particles (Fig. 42). On the contrary, the Bergmann fractured face cytoplasm exhibited a typical smooth surface and few isolated particles.

Climbing fiber-Purkinje spine synapses. With the SEM slicing technique, the teleost fish parent climbing fibers were observed approaching to the Purkinje cell soma (Fig.43) and then ascending toward the surface of the cortex, closely applied to the Purkinje primary trunk and secondary dendritic

Fig. 36. TEM of mouse cerebellar cortex. Glutaraldehyde-osmium tetroxide fixation. Alcian blue staining. Two "en passant" parallel fiber endings (PF) are observed synapsing with two longitudinally sectioned Purkinje dendritic spines (Ps).

Fig. 37. Freeze-etching replica of mouse cerebellar molecular layer showing a parallel fiber (PF)-Purkinje dendrite (Pd) spine synapse. The fractured parallel fiber "en passant" ending contains spheroidal synaptic vesicles (SV). Aggregate of intramembrane particles (arrow) are observed at the E face Purkinje spine postsynaptic membrane. The cleavage plane has intersected the synaptic cleft (arrowhead). The Bergmann glial cell cytoplasm (BG) partially ensheaths the spine synaptic contact.

Fig. 38. SEM fractograph of teleost fish Salmo trout processed by the freeze-fracture method. Several fractured parallel fiber varicosities (arrows) are observed in the vicinity of a spiny Purkinje dendritic branchlet (Pd). In spite of the low resolution SEM, the three-dimensional morphology of spheroidal synaptic vesicles is illustrated within the parallel fiber synaptic varicosities. The synaptic vesicles appear clustered by a homogeneous extravesicular substance.

Fig. 39. Freeze-etching replica of mouse cerebellar molecular layer illustrating two fractured parallel fiber-Purkinje spine synapses. At the upper part of the figure, the parallel fiber ending (PF) appears covering the fractured Purkinje spine (Ps). Pits and aggregation of intramembrane particles are observed (arrows) at the Pf postsynaptic membrane. The outer parallel spine synapse is observed at the center of the figure (arrowheads). The cytoplasmic fracture face of parallel fiber ending contains scarce spheroidal synaptic vesicles and randomly distributed intramembrane particles. At the lower part of the figure the cytoplasmic fracture face of Bergmann glial cells (BG) is noted.

Fig. 40. TEM of mouse cerebellar cortex. Glutaraldehyde-osmium tetroxide fixation. Two parallel fiber (PF)-Purkinje spine (Ps) synapses have been cross sectioned. The bulbous spine ends invaginate the parallel fiber presynaptic varicosities, which contain spheroidal, clear synaptic vesicles. The Bergmann glial cytoplasm (BG) ensheaths the invaginated spine synapses.

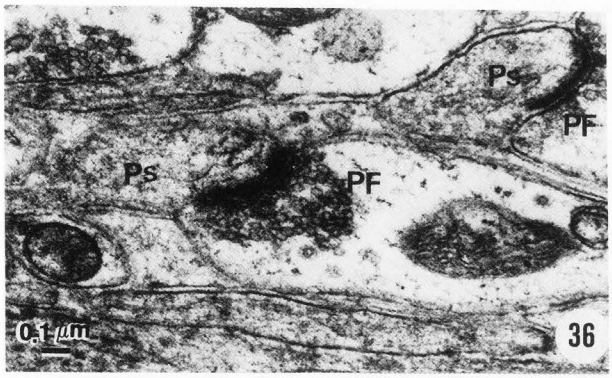
Ps
PF
Ps
PF
0.1 µm
36

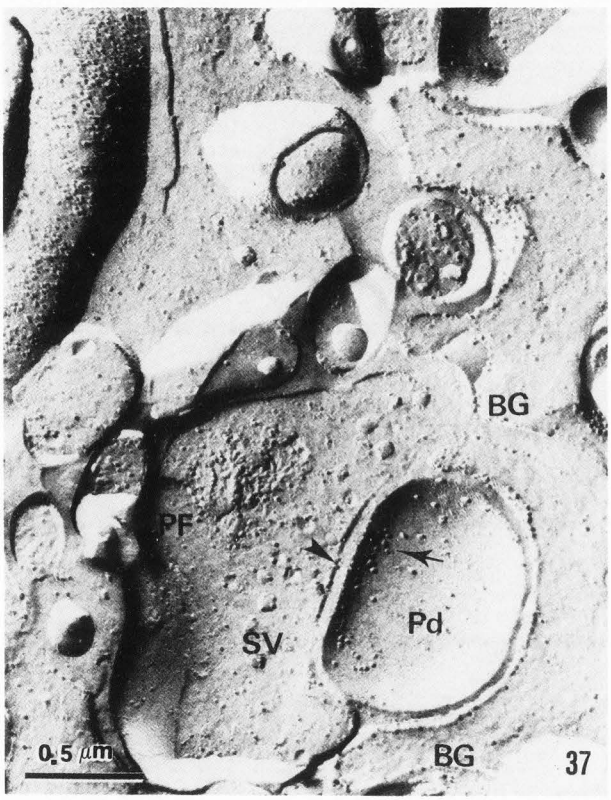
BG
PF
SV
Pd
0.5 µm
BG
37

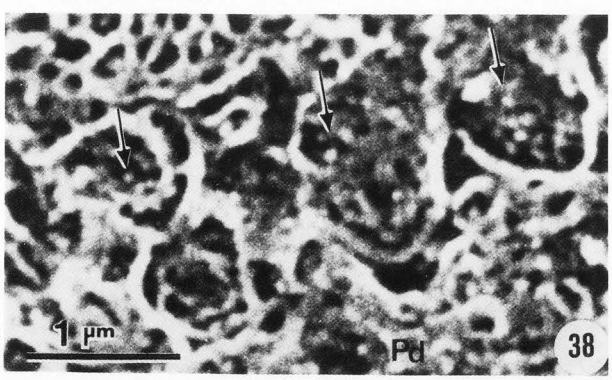
1 µm
Pd
38


BG
PF
BG
PF
Ps
BG
0.5 µm
39

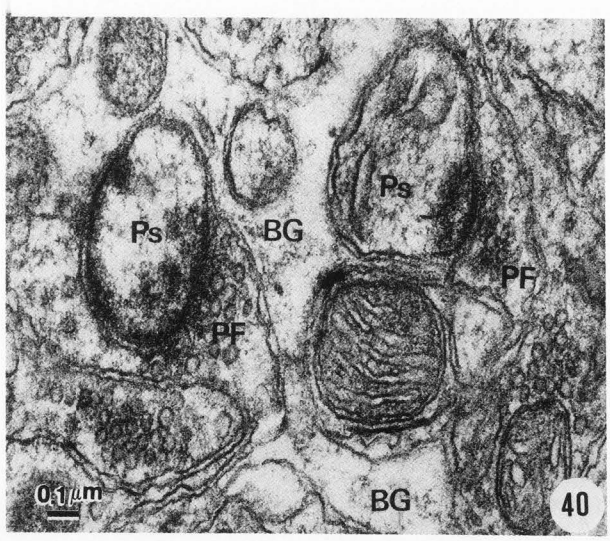
Ps
Ps
BG
PF
PF
0.1 µm
BG
40

branches. With the ethanol-cryofracturing technique, the climbing fibers of human cerebellum showed, as in the granular layer, an arborescence pattern type of bifurcation, characteristically spreading in three different planes (Fig. 44). In addition, collateral branches (Scheibel's collaterals) were observed extensively running in the molecular layer (Fig. 45). By means of SEM freeze-fracture method, the teleost fish terminal climbing fibers were seen ending by fine tendrils on the Purkinje spiny dendritic branches (Fig. 46).

In freeze-fracture replicas of mouse cerebellar molecular layer, fractured in a sagittal plane (Fig. 47), the climbing fiber endings were positively identified by: a) their large size in comparison with the parallel fiber endings; b) a dense packing of synaptic vesicles, and c) the formation of axospinodendritic contacts with the large Purkinje dendritic spines. In such replicas, the climbing fiber varicosities were well displayed and appeared fractured in a plane parallel to the main axis of large Purkinje dendrites. The examination of the E face climbing fiber presynaptic membrane revealed elevated localized patches, which were correlated with synaptic active sites. They were characterized by clusters of 8-15nm intramembrane particles (IMPs), 3 to 5 randomly distributed membrane protuberances and pits or craters, with diameters of approximately 12-16nm. The elevated patches appeared surrounded by IMPs free membrane domains. At these regions, the fracture process usually continued by splitting the Purkinje spine postsynaptic membrane, exposing its P face and finally extending toward the enveloping Bergmann glial cell, which disclosed its P and cytoplasmic fracture faces. The P face Purkinje spine membrane was characterized by a high density distribution of IMPs. Usually the climbing fiber endings contact with several Purkinje spines.

Stellate neurons. Human cerebellar cortex specimens, processed for SEM by ethanol-cryofracturing technique, showed in a parasagittal fracture of the outer third molecular layer, superficial short-axon stellate neurons (Fig. 48), with round, ellipsoidal or fusiform somata. These superficial stellate cells are easily recognized, since they are the only neurons in the upper molecular layer (Fig. 49). The plane of the fracture also allowed us to identify the ascending Purkinje dendritic branchlets. Stellate neurons, Purkinje dendritic branchlets and parallel fibers are the main structural elements of the outer molecular layer. Basket cells and fewer stellate cells were also found in the middle and inner thirds of the molecular layer. By these criteria, numerous stellate cells were recorded in the outer third molecular layer. Three to five beaded dendrites radiated from the cell body toward the neighboring Purkinje dendrites or other stellate cells. The axon originated by way of a typical triangular shape axon hillock and, after a short initial segment, bifurcated into tenuous varicose collaterals. Short, ramified and beaded dendrites emerged from the cell somata, directed toward the passing bundles of parallel fibers.

Some larger stellate cells bore axons exhibiting a meandering course, short sectioned collateral branches and round enlarged endings. Neither the sections nor the fractures studied with the SEM allowed observation of their ascending or descending collaterals, classically described in light microscope Golgi impregnated material. The terminal arborization of the axons appeared as a delicate plexus that branched and rebranched over the Purkinje dendritic branchlets. Small varicosities could be seen along the course of the fine terminal axonic branches.

With the SEM freeze-fracture method, the teleost fish stellate neurons exhibited nuclear and cytoplasmic features which resembled those of granule cells (for details, see Castejón and Castejón, 1987). In addition, the freeze-etching replicas of mouse stellate neurons revealed the cytoplasmic and nuclear envelope fracture faces of these cells (Fig. 50). Scarcely fractured endoplasmic reticulum canaliculi and vesicles were observed dispersed throughout the cytoplasm. The nuclear pores were randomly distributed over the surface of the fractured nuclear envelope.

The fractured synaptic endings of stellate cell axons could be observed applied directly over the Purkinje dendritic shaft, making typical axodendritic synapses (Fig. 51).

Discussion

In the present study, the slicing technique for SEM, ethanol-cryofractography for SEM, SEM freeze-fracture method and freeze-etching technique have been used in conjunction to study the three-dimensional cytoarchitectonic arrangement of vertebrate cerebellar cortex. The results obtained have been compared with light and transmission electron microscope findings in order to achieve proper identification of cerebellar neurons and intracortical circuits. This study provides with modern methods, a three-dimensional view of known cerebellar organization and confirms and expands light and transmission electron microscope studies of vertebrate cerebellum. The contribution of the technical methodology applied in the present study will be discussed first.

Slicing technique for SEM.

By this technique, unrevealed or hidden surfaces of cerebellar cortex were exposed (Castejón

Fig. 41. SEM micrograph of teleost fish (Arius spixii) cerebellar cortex processed by the slicing technique showing the non-synaptic segments of parallel fiber bundles (PF) in the molecular layer. Remnants of neuroglial cytoplasm (NC) are observed separating the parallel fibers.
Fig. 42. Freeze-etching replica of mouse cerebellar molecular layer showing fractured non-synaptic segments of parallel fiber (PF) widely separated by intervening Bergmann glial cell cytoplasm (BG). The P face parallel fiber membrane exhibits numerous irregularly distributed intramembrane particles.
Fig. 43. SEM micrograph of teleost fish (Arius spixii) cerebellar cortex processed by the slicing technique. The climbing fibers (arrows) coming from the granular layer pass through the Purkinje cell (PC) layer and ascend toward the molecular layer.
Fig. 44. SEM micrograph of teleost fish (Arius spixii) cerebellar molecular layer processed by the slicing technique. The climbing fibers (CF) and their collateral processes show a sagittal compartmentalization between the Purkinje dendrites (Pd).

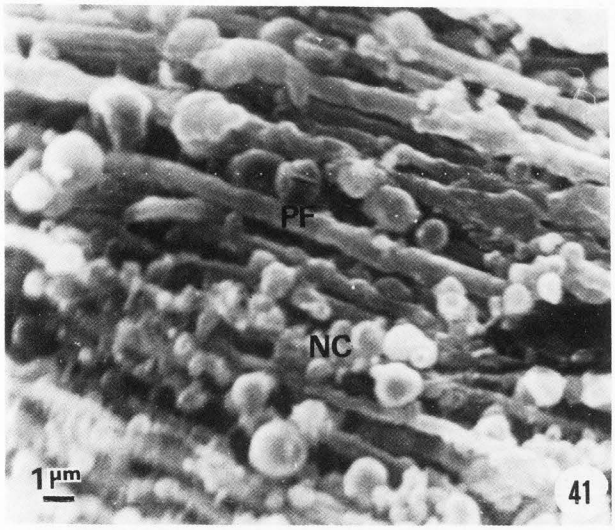
PF
NC
1 µm
41

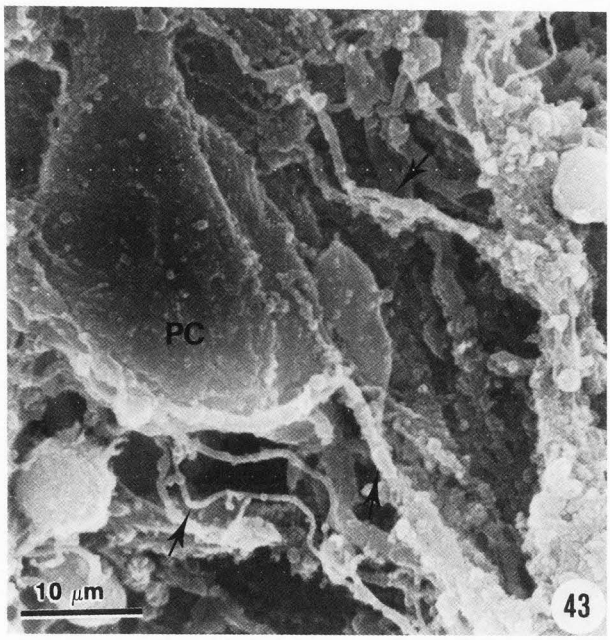
PC
10 µm
43

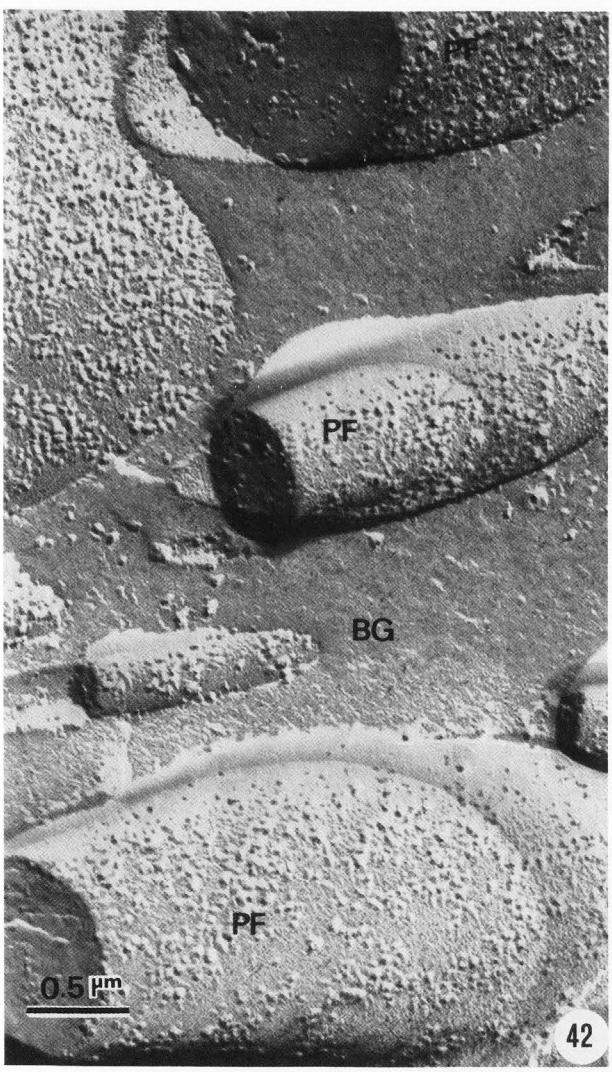
PF
PF
BG
PF
0.5 µm
42

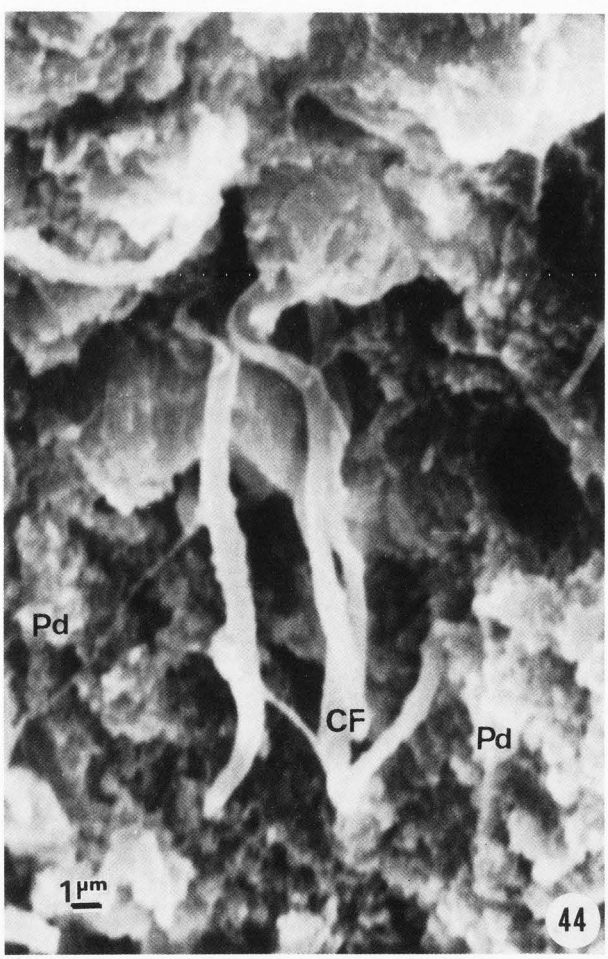
Pd
CF
Pd
1µm
44

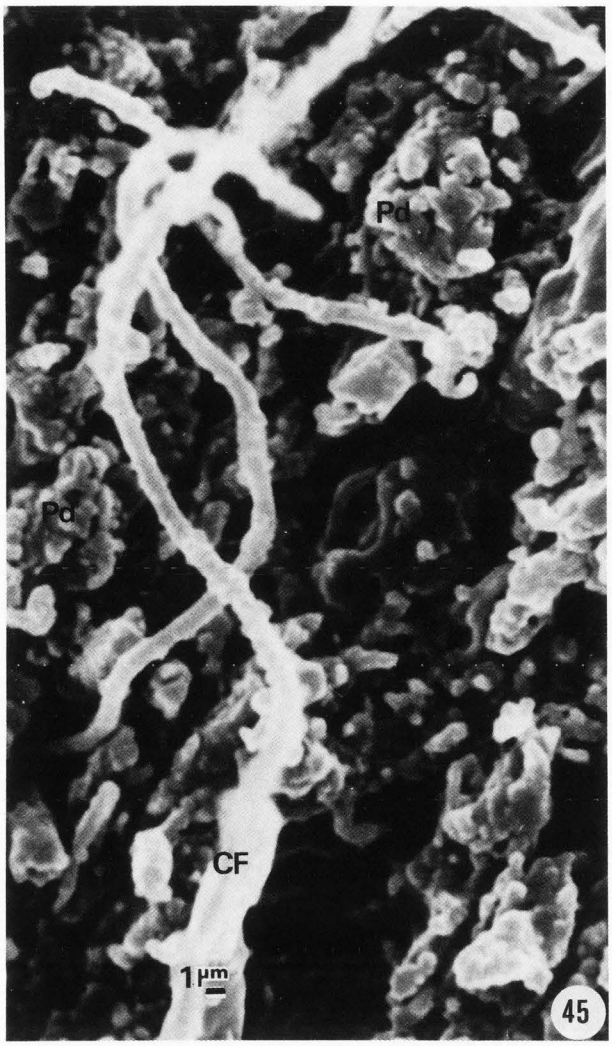
Pd
Pd
CF
1µm
45

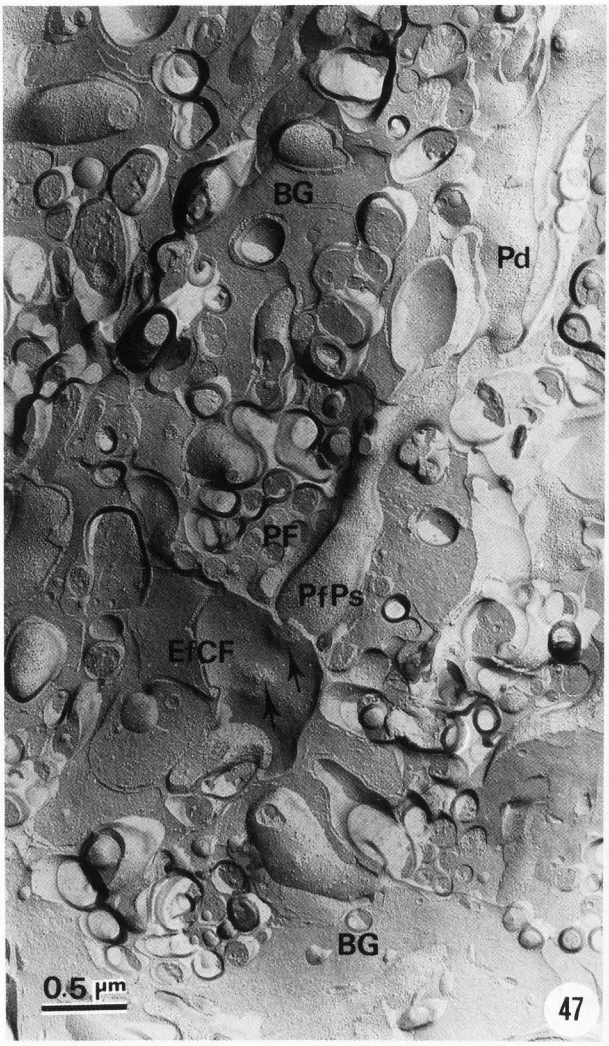
BG
Pd
PF
PfPs
EfCF
BG
0.5 µm
47

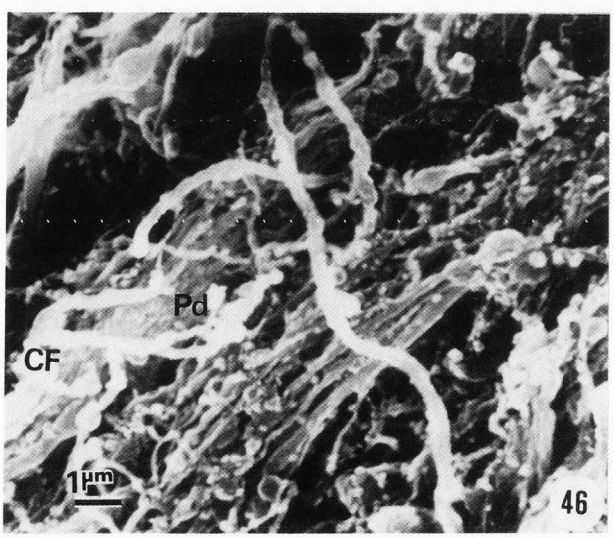
Pd
CF
1µm
46

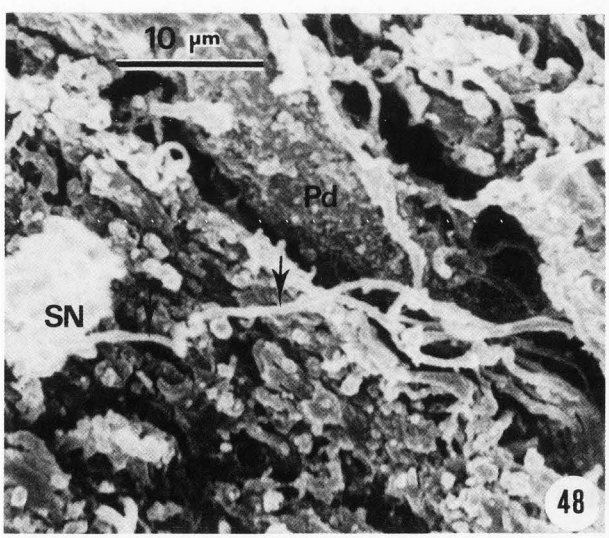
10 µm
Pd
SN
48

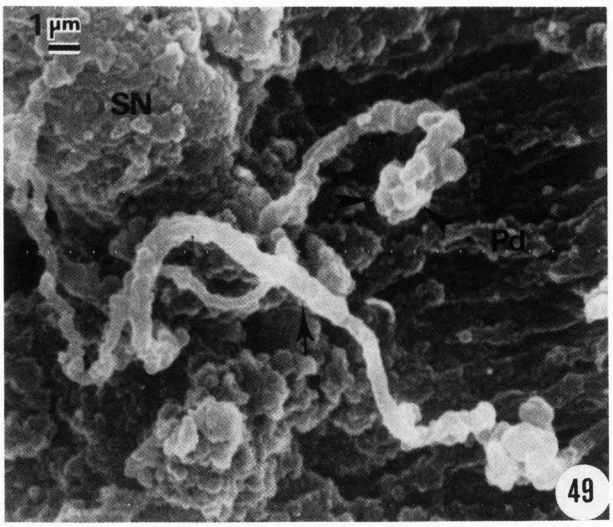

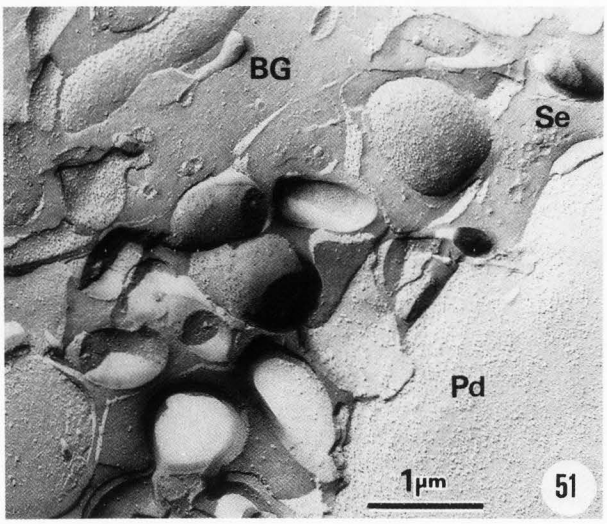

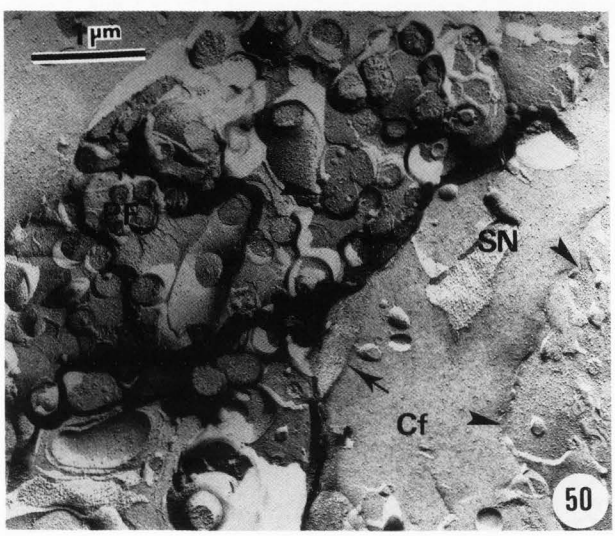

Fig. 49. SEM micrograph of teleost fish (Arius spixii) cerebellar outer molecular layer processed by the slicing technique. The stellate neuron (SN) shows a short dendrite (arrowheads) and a convoluted axon (arrow). Purkinje dendritic branchlets (Pd) are seen. Synaptic contacts are not distinguished.

Fig. 50. Freeze-etching replica of mouse cerebellar outer third molecular layer showing a stellate neuron (SN). The P face of plasma membrane (arrow), the cytoplasmic fractured face (Cf) and the P face of inner nuclear membrane (arrowheads) are visualized. The cross sectioned parallel fibers (PF) are also seen in the neighboring neuropil.

Fig. 51. Freeze-etching replica of mouse cerebellar outer third molecular layer. A stellate axonal ending (Se) appears attached directly to the shaft of the Purkinje dendritic branchlet (Pd). The intramembrane particle density of P face Purkinje dendritic membrane is observed. At the upper part of the figure, the Bergmann glial cell cytoplasm (BG) is seen.

and Caraballo, 1980a), thus allowing the observation of granule cells, mossy and climbing fiber glomeruli and Purkinje cells. These observations were later partially supported by the "creative tearing" technique (Scheibel et al., 1981) and the ultrasonic microdissection (Arnett and Low, 1985). In addition, a greater depth of exposed surface was achieved in certain areas by the "creative tearing" procedure, such as at the level of Purkinje cells and their synaptic relationship with basket cells and by ultrasonic microdissection at the level of Golgi cell and Purkinje dendritic spines.

Ethanol-cryofracturing technique.

Scanning electron microscopy combined with the cryofracture technique (Humphreys et al.,1974, 1975) has been of some potential value for studying the neuronal architecture and synaptic connections of the human cerebellar cortex (Castejón and

Fig. 45. SEM fractograph of human cerebellar molecular layer processed by the ethanol-cryofracturing technique. The climbing fiber (CF) and its Scheibel's collateral show the typical arborescence pattern type of bifurcation. Purkinje dendrite spiny branchlets (Pd) are observed in the close neighborhood.

Fig. 46. SEM micrograph of teleost fish (Arius spixii) cerebellar cortex processed by the slicing technique. Tendril collaterals of climbing fibers (CF) appear approaching to the fine, delicate Purkinje spiny branchlets (Pd) in the outer third molecular layer.

Fig. 47. Freeze-etching replica of mouse cerebellar molecular layer fractured in the sagittal plane. The cleavage plane has shifted from the E face climbing fiber ending (EfCF) to the P face Purkinje spine membrane (PfPs). Aggregate of intramembrane particles (arrows) and pits are observed at the climbing presynaptic membrane. The Purkinje spine appears connected by a long stalk to the parent dendrite (Pd). Cross cut parallel fiber (PF) and Bergmann glial cell (BG) are observed in the neuropil.

Fig. 48. SEM fractograph of human cerebellar molecular layer processed by ethanol-cryofracturing technique. The stellate neuron (SN) shows a short filiform axon (arrow) directed toward the Purkinje dendrite (Pd).

Caraballo, 1980b). This technique seems ideally suited for tracing intracortical cerebellar circuits and less convenient for studying outer nerve cell soma surface. For example, it allowed us to trace almost completely the intracortical course of climbing fibers. Similar results have not been obtained thus far with other techniques designed to facilitate SEM study of nerve tissue hidden surfaces.

The fracture of human cerebellar fragments, after freezing with liquid nitrogen (medium freezing rate) permitted the exploration of granule, Purkinje and molecular layers of cerebellum (Castejón and Valero, 1980). The fracture line isolated some cell types, such as granule and Golgi cells. In addition, a cryodissection of afferent fibers (mossy and climbing fibers), cerebellar cortex intrinsic fibers (parallel fibers, Golgi, basket and stellate cell axons) and most dendritic processes is produced. Apparently the nerve processes are kept intact due to the freezing of the ethanol impregnated tissue (Humphreys et al., 1975) which is transformed into an amorphous solid, which in turn acts as a solid matrix supporting the delicate neuronal processes.

After freezing with liquid nitrogen, the fracture of the cerebellar fragments is produced at the sites of tissue weakness, represented in the granular layer by the neuroglial cells, which partially surround the granule cell groups and the cerebellar glomeruli, and by the Bergmann glial cells in the Purkinje cell and molecular layers. The cerebellar neuroglial cells are thus partially removed by the cryofracture process. This fact explains the infrequent observation of neuroglial cells in the fractograph of the granular layer and the presence of large crevices at the sites previously occupied by the Bergmann glial cell bodies in the Purkinje cell layer. The Bergmann glial cells are astrocytic in nature and presumably represent a water-ion compartment easily detached during the cryofracture process. The removal of glial cells has been also reported by Lewis (1971). It is important to emphasize that with this technique we did not obtain internal details of cerebellar nerve cells, as those reported by Humphreys et al. (1974, 1975) in kidney and liver tissues.

A supportive technique, the Golgi light microscope technique, was used by us to correlate the findings obtained by the cryofracturing SEM procedure. The Golgi technique provides, with unsurpassed clarity and faithful delineation, the shape and spatial arrangements of isolated nerve units. This technique is indispensable for defining the matrix within which, data from ethanol-cryofracturing technique and freeze-fracture SEM can be interpreted. It is obvious that the new information obtained from these latter techniques can become useful only if it can be related to known structural entities such as cerebellar neurons and their intracortical circuits. In a previous paper we partially achieved this goal in relation with mossy fiber-granule cell synapses (Castejón, 1981). The image of tangled and overlapping neural processes produced by both techniques at different levels of resolutions and magnifications, demand an increasing effort to systematically correlate the results obtained with the combination of these techniques.

Freeze-fracture scanning electron microscopy.

Some internal details of fractured cerebellar nerve and neuroglial cells have been three-dimensionally viewed by SEM (Castejón, 1984) taking advantage of the washing out of soluble proteins from the fracture face induced by the freeze-fracture process (Haggis and Phipps-Todd, 1977). The neuronal and neuroglial nuclear chromatin observed by SEM could be well correlated with their TEM images, in which large heterochromatin masses could be seen. Since cerebellar tissue is primarily fixed with chemical fixatives, by perfusion or immersion techniques, an adequate preservation of chromatin material is expected. However, a certain degree of shrinkage and clumping of heterochromatin anastomotic bands was observed, which could be a denaturing reaction induced by the Freon freezing process. Chromatin fibers, as described by Haggis and Bond (1979) and Iino and Nagay (1981) in non-nervous tissue, were not observed in cerebellar nerve cells.

An interesting contribution of the freeze-fracture method for SEM, is also the three-dimensional visualization of the spatial arrangement and organization of endoplasmic reticulum surface. In general, fractured cerebellar nerve cells showed a caveolar appearance, presumably due to any one of the following possibilities. In single cells as also in multicellular systems, injury and cell death have been correlated with intracellular ice formation. In smooth muscle, an ideal model system for the investigation of cryoinjury, ice cavities and shrinkage of perinuclear region have been reported by Hunt et al. (1982). The cytoplasmic damage observed in some cerebellar neurons would be probably due to spherulytic crystalline formation (Luget, 1970). Apparently, a center of crystallization is formed in the cytoplasmic matrix, which while growing, rejects the endoplasmic reticulum and cell organelles. Another alternative is a cytoplasmic injury produced during rewarming and thawing by a process of devitrification, melting or recrystallization. Since fragments of cerebellar tissue were plunged into Freon at -150°C (rapid freezing rate), there is the likelihood of intracellular freezing with cooling velocity of damage from recrystallization of intracellular ice during warming. However, in our experiments, water in tissue was replaced by absolute ethanol prior to freezing, thus preventing ice crystal formation. Previous experiments of Humphreys et al. (1975) on liver; and Haggis et al. (1976) on muscle, suggest that in fixed tissues, ethanol freezes to a glass or non-crystalline state, both, at rapid freezing rates (tissue plunged into Freon at -150°C) or medium freezing rates (tissue plunged directly into liquid nitrogen) with no distortion of tissue structure. However, in tables of Physical Constants, the melting point of ethanol is given as -112°C to -117°C; so, it is possible that ethanol may crystallize below these temperatures, thereby producing some structural rearrangement similar to that produced by ice formation (G. Haggis, personal communication).

Freeze-etching technique.

The correlative study of freeze-etching replicas and freeze-fracture technique for SEM can greatly extend the visualization and understanding of the three-dimensional organization of cerebellar

nerve cells, especially the assembly of synaptic contacts. The replicas, by providing vistas of cleaved surfaces with higher resolution than that obtained at SEM level, enable the appreciation of the extent and three-dimensional configuration of synaptic membrane contacts. Its principal advantage is that, in addition to the intramembrane structure, it explores three-dimensional details not made visible by other techniques at cellular and macromolecular levels. By comparing with the freeze-fracture SEM images, complementary information and a more accurate view of the three-dimensional structure of cerebellar nerve cell was obtained (Castejón, 1984, 1986). Qualitative and quantitative freeze-etching analyses of mature and developing cerebellar cortex have been performed on certain regions, such as granule cells, mossy fiber, climbing fibers, Purkinje cells and Bergmann glial cells (Palay and Chan-Palay, 1974; Landis and Reese, 1974; Korte and Rosenbluth, 1980; García-Segura and Perrelet, 1982, 1984; García-Segura, 1985; Castejón, 1984; Castejón and Castejón, 1987). These investigations have provided basic information on the three-dimensional structure of cerebellar nerve cells and have revealed the specific distribution of intramembrane particles at pre- and post-synaptic sites.

Contribution of SEM to the Cytoarchitectonic study of Cerebellar Cortex

Granule Cell Layer

Granule cells. The present study shows the three-dimensional view of the outer surface and the interior of cerebellar granule cells and their processes as visualized by low resolution SEM and freeze-etching replicas. The freeze-fracture method for SEM allows direct access to the interior of granule cell, as well as preservation of some delicate structures such as cytoplasmic strands and cell organelles (Castejón, 1984). On the basis of configuration and spatial relationships, we have interpreted the cytoplasmic strands, running from the nucleus to the plasma membrane, as the genuine cytoplasmic components of the endoplasmic reticulum. Similar cytoplasmic strands have been observed by Haggis and Phipps-Todd (1977) in freeze-fractured chicken erythrocytes. In addition, TEM studies of several vertebrate cerebellar granule cells (Gray, 1961; Dahl et al., 1962; Fox, 1962; Castejón, 1969; Mugnaini, 1972; Palay and Chan-Palay, 1974), have reported a meager cytoplasm containing few tubules of rough and smooth endoplasmic reticulum, often confluent with the nuclear envelope by one side or the plasma membrane by the other one. However, high resolution SEM should be used in the future to characterize granule cell endoplasmic reticulum membranes on the basis of their membrane surface characteristics.

At the freeze-fracture SEM level there was also preliminary identification of cell organelles, (Castejón, 1981, 1984) such as mitochondria, lysosomes and the Golgi complex, according to their shape, size and intracytoplasmic localization. Mitochondria were mainly identified by their sausage-like shape, since mitochondrial cristae could not be disclosed by the freeze-fracture technique for SEM.

As previously reported (Castejón, 1984), the Golgi apparatus is characterized as a mass network containing large vacuoles and small vesicles, which closely resemble the schematic drawings from transmission electron micrograph reconstruction. Our scanning electron micrograph of the Golgi complex closely resembles the SEM appearance of the Golgi apparatus shown by Tanaka et al., (1976) in the rabbit pancreatic cell using the ion-etched technique, and by Sturgess and Moscarello (1976) in subcellular fractions isolated from rat liver cells, and could be easily correlated with TEM descriptions of Novikoff (1967).

The three-dimensional structure of chromatin observed in the fractured granule cell nucleus (Castejón, 1981) resembles chromatin in freeze-fractured chicken erythrocytes (Haggis and Bond, 1979). The SEM image of chromatin suggests that the granule cell is a good model for the study of heterochromatin in an interkinetic nucleus. The freeze-fracture method permitted us to observe the rough outer surfaces of the nuclear envelope. Some tubules were observed attached to the outer surface of the nuclear envelope, revealing that the freeze-fracture method preserves cytoskeletal components. However, we have not seen any clear evidence of nuclear pore structures, presumably due to the low resolution of SEM. As demonstrated by Kirschner et al. (1977) by high resolution SEM, visualization of the pore structure requires Triton X 100 pretreatment. Granule cell processes were traced in both, the granular and molecular layers.

Mossy fibers and mossy fiber glomeruli. In the granular layer we have identified, with the aid of the Golgi technique (Castejón, 1981), the mossy fibers with their typical rosette formations. Similar studies have been reported in other vertebrates by several authors (Cajal, 1926, 1955; Fox et al., 1967; Palay and Chan-Palay, 1974). In accordance with their light microscopic features, we have looked for mossy fibers at SEM level, following their course between the granule cell groups. We have characterized as mossy fibers those afferent fibers exhibiting rosette expansions. Such synaptic enlargements are not displayed by either climbing fibers or descending Purkinje cell axons (Castejón and Caraballo, 1980a). The only source of confusion arises between the fine beaded collaterals of Golgi axons and fine mossy branches forming small glomeruli. In such cases, only the continuity with the thick parent mossy fiber branches permitted a clear differentiation between the two types of fibers. At SEM level, the synaptic junctions between the mossy fiber and granule cell dendrites at the mossy glomerulus appeared as the contact surface between the smooth surface rosette expansion and several granule cell dendritic tips or dendritic claws (Castejón and Valero, 1980; Castejón, 1981).

With SEM slicing technique a clear distinction between fish mossy and climbing glomeruli could be made (Castejón and Caraballo, 1980a; Castejón, 1981). The mossy glomeruli are polygonal or round in shape, while the climbing glomeruli are thin elongated structures. The contact surface between the mossy fiber and granule cell dendrites was first described at SEM level by Castejón and Valero (1980) in human cerebellum using the ethanol-cryofracturing technique. A detailed view of the outer surface of the mossy glomerulus was

recently given by Scheibel et al. (1981). More recently additional information was reported by Arnett and Low (1985) using ultrasonic microdissection. Some inner features of fractured mossy glomerulus were for the first time reported in fish teleostean cerebellar cortex using the freeze-fracture method (Castejón, 1981).

The appearance of the mossy fiber glomerulus can be correlated with the stereodiagram shown by Eccles et al., (1967). The SEM observations of mossy fiber glomeruli offered additional information about the quantitative relations between granule cells and glomeruli. As illustrated in Fig.15, up to 18 granule cells have been observed surrounding one glomerulus. This 18:1 ratio is considerably higher than that (4.5:1) previously reported to occur in the vermis of adult cat (Eccles et al., 1967). About 17 dendrites have been observed entering the mossy glomerulus. This finding is in accord with the observation made by Fox et al.(1967) that up to 15 granule dendrites could enter the same glomerulus.

As shown in Fig. 13, the mossy fibers establish several "en passant" synapses with the granule cell dendrites of different glomeruli. The passage character of this synaptic relationship is a well known feature of mossy fiber branches (Eccles et al., 1967; Palay and Chan-Palay, 1974). Some mossy fiber glomeruli showed remnants of glial cytoplasm which were not observed in the climbing fiber glomeruli. Such observations are in full agreement with previous transmission electron microscope findings (Palay and Chan-Palay, 1974).

Climbing fibers and climbing fiber glomeruli. The SEM study of climbing fibers confirms and extends the basic morphological aspects of these fibers as earlier known from the pioneering Cajal (1955) classical account to the more recent studies of Carrea et al. (1947), Scheibel and Scheibel (1954), Szentagothai and Rajkovits (1959), Larramendi and Victor (1967), O'Leary et al. (1968, 1971), Fox et al. (1969), Chan-Palay and Palay (1970, 1971), Palay and Chan-Palay (1974), Murphy et al. (1973), Rivera-Domínguez et al. (1974) and Freedman et al. (1978). Critical problems regarding the proper identification of climbing fibers in the electron microscope have proved to be more difficult than their appearance under the light microscope would indicate. These problems were well documented by Chan-Palay and Palay (1970,1971) and Mugnaini (1972).

Climbing fibers were distinguished by their size, location, shape, course and known synaptic relationship. In a previous work (Castejón, 1983), we have visualized and characterized for the first time by SEM, the climbing fiber wavy pathway through the cerebellar cortex. As previously described by Chan-Palay and Palay (1971) in camera lucida observations, we have traced fine collateral branches that leave the white matter and enter the granular layer. However, SEM cryofracture did not give a complete view of the plexoid cluster of axon collaterals lying between white matter and the ganglionic layer as described by Murphy et al. (1973) using Golgi impregnation technique.

The climbing fibers have been described by light microscopy as having thin segments and fusiform enlargements; however silver staining fails to reveal these enlargements (Larramendi, 1968). In our studies, we have not observed such fusiform expansions. The identification of climbing fiber at TEM level has been a matter of controversy in the last two decades. They were described as making synaptic contacts directly upon the smooth surface of the Purkinje dendritic shaft. However, more recently Larramendi and Victor (1967) and Chan-Palay and Palay (1970) established that climbing fibers make spine synapses with the Purkinje dendritic branches. Our studies (Castejón, 1986) tend to agree with these latter observations. However, additional work is needed at the SEM level in order to fully support this concept.

As Cajal (1955) has shown, the climbing fiber increases in complexity as the phylogenetic scale is ascended. However, the basic structure and connections remain the same in all the species (Scheibel and Scheibel, 1954). The morphological separability of climbing fibers from other axonal substrates and the cross-over which follows branching, as described in the present paper, are features which have also been observed by O'Leary et al. (1971) during the histogenesis of the rat cerebellar climbing fibers.

With SEM it is possible to estimate with a more reliable degree of certainty the amount of branching of climbing fiber in the granular and molecular layers. This subject has been a matter of controversy in the past. Cajal (1955) did not report climbing fiber collaterals in the granular layer. They were first described by Scheibel and Scheibel (1954) as retrograde collaterals descending from the molecular layer. More recently a detailed account of climbing fiber bifurcation in the granular layer was made by Fox et al. (1969) and Chan-Palay and Palay (1971). In the present study a higher incidence of branching of climbing fiber was detected in the granular layer. We have distinguished two types of climbing fiber ramifications: the glomerular collaterals and the tendril collaterals. The first ones form the climbing fiber glomeruli, supporting the Palay and Chan-Palay (1974) TEM descriptions. The tendril collaterals appeared surrounding the granule cell groups, but their mode of ending was not ascertained.

Golgi cells. We have identified Golgi cells in the granular layer at SEM level (Castejón and Valero, 1980) by their large size, two differently orientated dendritic processes and typical highly branched axonal ramifications, according to earlier descriptions given by Retzius (1891), Cajal (1955) and more recently by O'Leary et al. (1968), Sotelo (1969), Uchizono (1969), Hillman (1969) and Castejón (1976). The soma and processes of Golgi cells were also disclosed at SEM level by ultrasonic microdissection (Arnett and Low, 1985).

The Golgi cell axonal plexus was observed participating in the formation of mossy and climbing fiber glomeruli. The beaded aspect of Golgi axonal ramifications, as seen with the Golgi light microscope and TEM, permits their identification with the scanning electron microscope. However, in some electron micrographs they can be confused with tendril collaterals of climbing fibers or with the fine varicose branches of mossy fibers (Castejón and Caraballo, 1980a).

The synaptic contacts between Golgi axonic endings and granule cell dendrites are formed by a 1:1 ratio. In this case, as demonstrated in

Fig. 24 by the SEM freeze-fracture method, a fine beaded Golgi axonal ramification establishes contact with a granule cell dendritic tip. This synapse has been previously described by light microscopy and TEM studies (Fox et al., 1967; Palay and Chan-Palay, 1974; Castejón, 1976). The localization of this cell within the granular layer limits the SEM study of their synaptic relationships in both granular and molecular layers even using techniques for exposing hidden surfaces.

Purkinje Cell Layer

As previously mentioned, with the slicing and ethanol-cryofracturing techniques, removal of Bergmann glial cells was observed at the Purkinje cell layer. A certain vulnerability of this layer to ultrasonication has been reported by Arnett and Low (1985). The Purkinje cell outer surface was better preserved in experimental material, the teleost fishes, using the slicing technique, than in human pathological samples applying the ethanol-cryofracturing technique. In teleost fish we have used glutaraldehyde fixation by perfusión, which appears to give better results than the glutaraldehyde-immersion fixation utilized in human cerebellar preparations.

With the ethanol-cryofracturing technique a partial visualization of supra- and infra-ganglionic plexuses of Purkinje cell was obtained (Castejón and Valero, 1980). Neuroglial cells at this layer were scarcely preserved. With the freeze-fracture SEM we have observed only in Salmo trout cerebellar cortex some vestiges of Bergmann glial cell cytoplasm applied to Purkinje cell dendrites. With the slicing and ethanol-cryofracturing techniques the basket cell axosomatic synapses and climbing fibers were also observed at the Purkinje cell layer (Castejón and Valero, 1980; Castejón and Caraballo, 1980a,b).

Prominent features of this layer have been obtained by Scheibel et al. (1981) with the creative tearing technique. Basket cell axonic collaterals closely applied to the Purkinje cell body, ascending climbing fibers and neuroglial cells were visualized. Ultrasonic microdissection has also allowed a beautiful picture of basket cell body with their processes directed toward the Purkinje cell soma (Arnett and Low, 1985). An additional SEM study of Purkinje pericellular basket will be required in order to have a better three-dimensional picture of this structure and an appropriate correlation with the images obtained by the Golgi light microscopy (Fox et al., 1967) and transmission electron microscopy (Palay and Chan-Palay, 1974).

Molecular Layer

The scanning electron microscopic observations of the Purkinje dendrite-parallel fiber synaptic contacts, made by means of ethanol-cryofracturing technique and the freeze-fracture method confirmed their "en passant" cruciform arrangement earlier described by Golgi (1873), Cajal (1955) and Fox and Barnard (1957) and subsequently by Gray (1961), Hamori and Szentagothai (1964), Castejón (1968) and Palay and Chan-Palay (1974).

The fractured "en passant" endings of parallel fibers were seen containing spherical synaptic vesicles. The visualization of the interior of these synaptic varicosities gives the freeze-fracture method for SEM some potential value for studying synaptic morphology at higher SEM resolution power.

The study of climbing fibers in the molecular layer was facilitated by the removal of Bergmann glial cell by the ethanol-cryofracture process. This neuroglial covering was earlier mentioned by Hamori and Szentagothai (1964) as an obstacle for visualizing climbing fibers at this level. In both the granular and molecular layers, we searched for axo-axonic connections of climbing fibers with mossy fiber, stellate and basket cell axons and parallel fibers. The existence of this type of synapses has been reported by Scheibel and Scheibel (1954). However until now, we have not found evidence of such axo-axonic contacts. TEM studies (Chan-Palay and Palay, 1970) have also failed to reveal such specialized contacts. The SEM images of climbing fibers obtained by the slicing technique also supported the parasagittal compartmentalization of climbing fibers as postulated by Freedman et al. (1978).

In addition, SEM slicing and ethanol-cryofracturing techniques offer the advantages of following the tortuous course and extreme tenuity of climbing tendril collaterals in the molecular layer, overcoming the inherent difficulties derived from the interpretation of TEM fine section studies. Larramendi and Victor (1967) have shown that climbing fibers synapse on thorns emitted from the so-called smooth branches of the Purkinje dendritic tree, and not directly upon the dendritic shaft according to the classical descriptions of Cajal (1955). The SEM observations of climbing fibers at the molecular layer clearly showed that these fibers are not really attached to the Purkinje dendritic trees but separated by an interspace, supporting the Larramendi and Victor (1967) TEM study.

Because of its ability to disclose protein moieties at the synaptic membranes, freeze-etching technique permitted the visualization of internal details of typical excitatory synapses such as the climbing fiber-Purkinje spine synapses and parallel fiber-Purkinje spine invaginated synapses. An aggregation of intramembrane particles at the P face of presynaptic membrane as well as vesicles attachment sites were seen. These membrane features are in accordance with the characteristic presynaptic specializations at excitatory synapses (Pfenninger et al., 1972; Sandri et al.,1972; Landis and Reese, 1974; Rash and Ellisman,1974; Venzin et al., 1977; Tokunaga, 1979; Korte and Rosenbluth, 1980; Hama, 1980; Raviola and Raviola, 1982; García Segura and Perrelet, 1982, 1984). In addition, the freeze-etching technique provides further information on Bergmann glial relationship with parallel and climbing fibers and on the synaptic relationship of climbing fiber-Purkinje dendrites. Such three-dimensional information at a higher level of resolution, has not been provided by any other technique thus far applied to the study of cerebellar molecular layer. As shown in the present paper, the cleavage planes obtained through the spine synapses permitted us to obtain a better spatial relationship and new information on macromolecular assembly of pre- and post-synaptic structures.

The SEM observations on stellate neurons have been correlated wherever possible with the classical description of stellate cells made by optical and electron microscopes (Castejón and Castejón, 1987). However, further SEM and freeze-etching

studies are needed in order to three-dimensionally explore the synaptic relationship with climbing and parallel fibers and other stellate cells.

Acknowledgement

This work has been partially supported by CONICIT (Project #S1-1251) and by CONDES-LUZ.

The author wishes to express his appreciation to Rafael Espinoza and Nelly Montiel for their skillful technical assistance and Ralph Casperssen for the photographic work.

References

Anderson TF (1951) Techniques for the preservation of three dimensional structures in preparing specimens for the electron microscope. Trans NY Acad Sci 13, 130-134.

Antal M (1977) Scanning electron microscopy of photoreceptors. Ophtalmologica (Basel) 174, 280-284.

Arnett CE, Low FN (1985) Ultrasonic microdissection of rat cerebellum for scanning electron microscopy. Scanning Electron Microsc. 1985; I: 247-255.

Boyde A, Wood C (1969) Preparation of animal tissues for surface scanning electron microscopy. J Microscopy 90, 221-249.

Bredberg G (1979) Scanning electron microscopy of nerves within the Organ of Corti. Arch Oto-Rhino-Laryng 217, 321-330.

Cajal SR (1926) Sur les fibres mousseuses et quelques points douteux de la texture de l'ecorce cérebélleuse. (On the mossy fibers and some doubtful points on the texture of the cerebellar cortex) Trab Lab Invest Biol (Madrid) 24, 215-251.

Cajal SR (1955) Cervelet. Structure de l'ecorce cérebélleuse. In: Histologie du Systeme Nerveux de l'Homme et des Vertébres. (The Cerebellum. Structure of the Cerebellar cortex. In: Histology of the Central Nervous System of Man and Vertebrates). Vol. II. Consejo Superior de Investigaciones Científicas. Instituto Ramón y Cajal. Madrid. pp. 42-54.

Cajal SR, De Castro F (1972) In: Elementos de Técnica Micrográfica del Sistema Nervioso. (Elements of Micrographic Techniques of the Nervous System). Edit Salvat. Barcelona. pp. 65-88.

Carrea RME, Reissig H, Mettler FA (1947) The climbing fiber of the simian and feline cerebellum: Experimental inquiry into their origin by lesions of the inferior olives and deep cerebellar nuclei. J Comp Neurol 87, 321-365.

Castejón OJ (1968) Observaciones microscópico-electrónicas a nivel de la capa molecular de la corteza cerebelosa. (Electron microscopic observations at the level of the molecular layer of the cerebellar cortex). Doctoral Thesis. Invest Clin 27, 57-108.

Castejón OJ (1969) Ultraestructura de la capa granulosa de la corteza cerebelosa humana. Organización de las células granulosas. (Ultrastructure of granular layer of human cerebellar cortex. Organization of the granule cells). Invest Clin 29, 29-46.

Castejón OJ (1971) Ultraestructura de los glomérulos cerebelosos humanos. (Ultrastructure of human cerebellar glomeruli). Invest Clin 38, 49-72.

Castejón OJ (1976) Ultraestructura de la célula de Golgi de la corteza cerebelosa. (Ultrastructure of the Golgi cells of the cerebellar cortex). Bol Acad Ciencias Fis Mat Nat 107, 67-110.

Castejón OJ, Morales DA, Caraballo AJ (1976) Light and scanning microscopic study of cerebellar cortex of teleost fishes (Arius spixii). Rev Micros Elec 3, 30-31.

Castejón OJ, Caraballo AJ (1980a) Light and scanning electron microscopic study of cerebellar cortex of teleost fishes. Cell Tissue Res 207, 211-226.

Castejón OJ, Caraballo AJ (1980b) Application of the cryofracture and SEM to the study of human cerebellar cortex. Scanning Electron Microsc. 1980; IV: 197-207.

Castejón OJ, Valero CJ (1980) Scanning electron microscopy of human cerebellar cortex. Cell Tissue Res 212, 363-374.

Castejón OJ (1981) Light microscope, SEM and TEM study of fish cerebellar granule cells. Scanning Electron Microsc. 1981; IV: 105-113.

Castejón OJ, Castejón HV (1981) Transmission and scanning electron microscopy and ultracytochemistry of vertebrate and human cerebellar cortex. In: Glial and Neuronal Cell Biology. Acosta Vidrio E, Fedoroff S (Eds). AR Liss, New York, pp 249-258.

Castejón OJ (1983) Scanning electron microscope recognition of intracortical climbing fiber pathways in the cerebellar cortex. Scanning Electron Microsc. 1983; III: 1427-1434.

Castejón OJ (1984) Low resolution scanning electron microscopy of cerebellar neurons and neuroglial cells of the granular layer. Scanning Electron Microsc. 1984; III: 1391-1400.

Castejón OJ (1986) Freeze-fracture features of fish and mouse cerebellar climbing fibers. In: Electron Microscopy 1986. Imura T, Maruse S, Suzuki T (Eds). J Electron Micros 35 (Suppl), 3165-3166.

Castejón OJ, Castejón HV (1987) Electron microscopy and glycosaminoglycans histochemistry of cerebellar stellate neurons. Scanning Microsc 1: 681-693.

Chan-Palay V, Palay SL (1970) Interrelations of basket cell axons and climbing fibers in the cerebellar cortex of the rat. Z Anat Enwickl Gesch 132, 191-227.

Chan-Palay V, Palay SL (1971) Tendril and glomerular collaterals of climbing fiber in the granular layer of the rat's cerebellar cortex. Z Anat Entwickl Gesch 133, 247-273.

Dahl V, Olsen S, Birch-Anderson A (1962) The fine structure of the granular layer in the human cerebellar cortex. Acta Neurol Scand 38, 83-97.

Eagleson GW, Malacinski GM (1986) A scanning electron microscopy and histological study of the effects of the mutant eyeless (e/e) gene upon the hypothalamus in the Mexican axolotl ambystoma mexicanum shaw. Anat Rec 215, 317-327.

Eccles J, Ito M, Szentagothai J (1967) The Cerebellum as a Neuronal Machine. Springer Verlag, New York. pp 215-219.

Estable-Puig RF, Estable-Puig JF (1975) Brain cyst formation: A technique for SEM study of the Central Nervous System. Scanning Electron Microsc. 1975; 282-286.

Fasekas I, Bácsy E, Rappay G (1978) Identification of epithelial cells and fibroblasts in hypophysis intermediate lobe cultures by scanning electron microscopy. Acta Biol Sci Hung 29,407-416.

Fox CA, Barnard JW (1957) A quantitative study of the Purkinje dendritic branchlets and their relationship to afferent fibers. J Anat (Lond) 91, 299-313.

Fox CA (1962) Fine structure of the cerebellar cortex. In: Correlative Anatomy of the Nervous System. Crosby EC, Humphreys T, Lauer EW (Eds). MacMillan Co. New York. pp 192-198.

Fox CA, Hillman DE, Siegesmund KA, Dutta CR (1967) The primate cerebellar cortex: A Golgi and electron microscopic study. Prog Brain Res 25, 174-225.

Fox CA, Andrade A, Schwyn RC (1969) Climbing fiber branching in granular layer. In Neurobiology of Cerebellar Evolution and Development. Llinas R (Ed). Chicago, AMAERF Institute for Biomedical Research. pp 603-611.

Freedman SL, Voogd J, Vielvoye J (1978) Experimental evidence for climbing fibers in the avian cerebellum. J Comp Neurol 15, 243-252.

García Segura LM, Perrelet A (1982) Climbing fiber destruction affects dendritic and spine membrane organization in Purkinje cell. Brain Res 236, 253-260.

García Segura LM, Perrelet A (1984) Postsynaptic membrane domains in the molecular layer of the cerebellum: A correlative between presynaptic inputs and postsynaptic plasma membrane organization. Brain Res 321, 255-256.

García Segura LM (1985) Trans-synaptic modulation of Purkinje cell plasma membrane organization by climbing fiber axonal flow. Exp Brain Res 6. 186-193.

Golgi C (1873) Sulla structura della sostanza grigia del cerebello.(On the structure of cerebellar gray matter). Gazz Med Ital 31, 244-246.

Gray EG (1961) The granule cells mossy synapses and Purkinje spine synapses of the cerebellum: Light and electron microscope observations. J Anat (Lond) 95, 345-356.

Haggis GH (1970) Cryofracture of biological material. Scanning Electron Microsc 1970; 97-104.

Haggis GH, Bond EF, Phipps-Todd B (1976) Visualization of mitochondrial cristae and nuclear chromatin by SEM. Scanning Electron Microsc 1976; I: 282-286.

Haggis GH, Phipps-Todd B (1977) Freeze-fracture of scanning electron microscopy. J Micros III, 193-201.

Haggis GH, Bond EF (1979) Three-dimensional view of the chromatin in freeze-fracture chicken erythrocyte nuclei. J Micros 115, 225-234.

Hama K (1980) Fine structure of the afferent synapses and gap junctions on the hair cell in the saccular macula of goldfish: a freeze-fracture study. J Neurocytol 9, 845-860.

Hamori J, Szentagothai J (1964) The "crossing-over" synapses: An electron microscope study of the molecular layer in the cerebellar cortex. Acta Biol Acad Sci Hung 15, 95-117.

Hansson HA (1970) Scanning electron microscopy of the rat retina. Z Zellforsch 107, 23-44.

Hartwig HG, Korf HW (1978) The epiphysis cerebri of poikilothermic vertebrates: A photosensitive neuroendocrine circumventricular organ. Scanning Electron Microsc 1978; II: 163-168.

Hillman DE (1969) Neuronal organization of the cerebellar cortex in amphibia and reptilia. In: Llinas R (Ed). Neurobiology of Cerebellar Evolution and Development. Am Med Assn/Educ & Res Fnd, Chicago. pp 279-325.

Humphreys WJ, Spurlock BO, Johnson JS (1974) Critical point drying of ethanol-infiltrated cryofractured biological specimens for scanning electron microscopy. Scanning Electron Microsc. 1974; 276-282.

Humphreys WJ, Spurlock BO, Johnson JS (1975) Transmission electron microscopy of tissue prepared for scanning electron microscopy by ethanol-cryofracturing. Stain Tech 50, 119-125.

Hunt CJ, Taylor MJ, Pegg DE (1982) Freeze-substitution and isothermal freeze-fixation studies to elucidate the pattern of ice formation in smooth muscle at 252 K (-21°C). J Micros 125, 177-186.

Iino A, Nagay S (1981) Chromatin and chromosome observed by scanning electron microscopy. Biomedical Res 2 (Suppl), 91-97.

Kessel RC, Kardon RH (1981) Scanning electron microscopy of mammalian neuroepithelia. Biomedical Res 2 (Suppl), 483-489.

Kirschner RH, Rusli M, Martin TE (1977) Characterization of the nuclear envelope, pore complexes, and dense lamina of mouse liver nuclei by high resolution scanning electron microscopy. J Cell Biol 72, 118-132.

Korte GE, Rosenbluth J (1980) Freeze-fracture study of the postsynaptic membrane of the cerebellar mossy fiber synapse in the frog. J Comp Neurol 193, 689-700.

Krstic RV (1974) Scanning electron microscopic study of the freeze-fractured pineal body of the rat. Cell Tissue Res 209, 129-135.

Lametschwandtner A, Simonsberg O, Adam H (1977) Vascularization of the pars intermedia of the hypophysis in the toad, bufo bufo (L.) (Amphibia, Anura). Cell Tissue Res 179, 11-16.

Landis D, Reese RS (1974) Differences in membrane structure between excitatory and inhibitory synapses in the cerebellar cortex. J Comp Neurol 155, 93-126.

Larramendi LMH, Victor T (1967) Synapses on the Purkinje cell spines in the mouse. An electron microscopic study. Brain Res 5, 15-30.

Larramendi LMH (1968) Morphological characteristics of extrinsic and intrinsic nerve terminals and their synapses in the cerebellar cortex of the mouse. In: The Cerebellum in Health and Disease. Fields WS, Willis WD (Eds). Warren H Green Inc. St. Louis. USA. 63-110.

Lewis RE (1971) Studying neuronal architecture and organization with the scanning electron microscope. Scanning Electron Microsc 1971; 283-288.

Low FN (1982) The central nervous system in scanning electron microscopy. Scanning Electron Microsc 1982; II: 869-890.

Luget BJ (1970) Physical changes occurring in frozen solutions during rewarming and melting. In: The Frozen Cell. Wolstenholme GEW, O'Connor M (Eds) J & A Churchill (Lond). pp 27-50.

Mannen H (1978) Three-dimensional reconstruction of individual neurons in higher mammals. Internat Rev Cytol (Suppl) 7, 329-372.

Matsuda S, Uehara Y (1981) Cytoarchitecture of the rat dorsal root ganglia as revealed by scanning electron microscopy. J Electron Micros 30, 136-140.

Merchant RE (1979) Scanning electron microscopy of spinal nerve exits of normal and BCG

infected dogs. Scanning Electron Microsc 1979; III: 341-345.

Messer A (1977) The maintenance and identification of mouse cerebellar granule cells in monolayer culture. Brain Res 130, 1-12.

Mitchell JA (1980) Scanning electron microscopy of brain ventricular surfaces. A bibliography. Scanning Electron Microsc 1980; III: 475-484.

Mugnaini E (1972) The histology and cytology of the cerebellar cortex. In: The Comparative Anatomy and Histology of the Cerebellum. Larsell O, Jansen J (Eds). The Human Cerebellum, Cerebellar Connections and Cerebellar Cortex. University of Minnesota, Minneapolis. pp 201-265.

Murphy MG, O'Leary KL, Cornblath D (1973) Axoplasmic flow in cerebellar mossy and climbing fibers. Arch Neur 28, 118-123.

Novikoff AB (1967) Enzyme localization and ultrastructure of neurons. In: The Neuron. Hyden H (Ed), Elsevier, New York. pp 255-318.

Obtsuki K (1972) Scanning electron microscopic studies on rabbit's spinal cord by resin cracking method. Arch Histol Jap 34, 405-415.

O'Leary JL, Petty JM, Smith MB, Inukai J (1968) Cerebellar cortex of rat and other animals. An ultrastructural study. J Comp Neurol 134, 401-432.

O'Leary JL, Inukai J, Smith MB (1971) Histogenesis of the cerebellar climbing fiber in the rat. J Comp Neurol 142, 377-392.

Palay SL, Chan-Palay V (1974) Cerebellar Cortex. Cytology and Organization. Springer-Verlag. Berlin, 1-348.

Pfenninger K, Akert K, Moor H, Sandri C (1972) The fine structure of freeze-fracture presynaptic membranes. J Ultrast Res 35, 451-475.

Phillips MI, Balhorn L, Leavitt M, Hoffman W (1974) Scanning electron microscope study of the rat subfornical organ. Brain Res 80, 95-100.

Privat A, Drian MJ, Mandon P (1973) The outgrowth of rat cerebellum in organized culture. Z Zellforsch 146, 45-76.

Rash JE, Ellisman MH (1974) Studies of excitable membranes. Macromolecular specializations of the neuromuscular junction and the nonjunctional sarcolemma. J Cell Biol 63, 567-586.

Raviola E, Raviola G (1982) Structure of the synaptic membranes in the inner plexiform layer of the retina: A freeze-fracture study in monkeys and rabbits. J Comp Neurol 309, 233-248.

Retzius G (1891) Kleine Mitteilungen aus dem Gebiete der Nervenhistologie. (Short communication on the nerve histology). Biolog Untersuch (Neue Folge) 4, 57-59.

Rivera-Domínguez M, Mettler FA, Novack CR (1974) Origin of cerebellar climbing fibers in the Rhesus monkey. J Comp Neurol 155, 331-342.

Saetersdal TS, Myklebust R (1975) Identification of nerve fibers in the scanning electron microscope. J Micros 103, 63-69.

Sandri C, Akert K, Livingston RB, Moor H (1972) Particle aggregation at specialized sites in freeze-etched postsynaptic membranes. Brain Res 41, 1-6.

Scheibel MD, Scheibel AB (1954) Observations on the intracortical relations of climbing fibers of the cerebellum. J Comp Neurol 101, 733-764.

Scheibel AB, Paul L, Fried I (1981) Scanning electron microscopy of the central nervous system: I. The Cerebellum. Brain Res Reviews 3, 207-228.

Seymour RM, Berry M (1975) Scanning and transmission electron microscope studies of interkinetic nuclear migration in the cerebral vesicles of the rat. J Comp Neurol 160, 105-125.

Siew S (1979) Scanning electron microscopy of the human spinal cord and dorsal root ganglia. Scanning Electron Microsc 1979; III: 421-429.

Silberberg DH (1975) Scanning electron microscopy of organotypic rat cerebellum cultures. J Neuropathol Exp Neurol 34, 189-199.

Sotelo C (1969) Ultrastructural aspects of the cerebellar cortex of the frog. In: Llinas R (Ed). Neurobiology of Cerebellar Evolution and Development. Am Med Assn/Educ & Res Fnd, Chicago. pp 327-371.

Sturgess JM, Moscarello MA (1976) Surface ultrastructure of the Golgi complex. Scanning Electron Microsc 1976; II: 145-152.

Szentagothai J, Rajkovits V (1959) Uber den Ursprung der Kletterfasern des Kleinhirns. (On the origin of cerebellar climbing fibers). Z Anat Entwickl Gesch 121, 130-141.

Tanaka K, Iino A, Naguro T (1976) Scanning electron microscopic observations on intracellular structures of ion-etched materials. Arch Histol Jap 39, 165-175.

Tokunaga A (1979) Increase of large intramembranous particles in the presynaptic active zone after administration of 4-aminopyridine. Brain Res 174, 207-211.

Uchizono K (1969) Synaptic organization of the mammalian cerebellum. In: Llinas R (Ed). Neurobiology of Cerebellar Evolution and Development. Am Med Assn/Educ & Res Fnd, Chicago. pp 549-583.

Venzin MG, Sandri K, Akert K, Wyss U (1977) Membrane associated particles of the presynaptic active zone in rat spinal cord. A morphometric analysis. Brain Res 130, 393-404.

Discussion with Reviewers

Reviewer I: From a practical standpoint, which technique(s) would you recommend to those studying the microanatomy of the cerebellum?

Author: I would recommend the SEM slicing technique and the ethanol-cryofracturing technique, especially for those interested in tracing neuronal circuits and studying cytoarchitectonic arrangement. They are relatively easy and simple SEM techniques for neuroanatomy. In all cases, they should be used in conjunction with the Golgi technique for light microscopy for proper identification of neuronal cell types, afferent and efferent fibers.

Reviewer II: Were studies in human cerebellum limited to SEM?

Author: Since twenty years ago we have been carrying out a systematic transmission electron microscope study of human cerebellar cortex of patients with brain tumors, congenital malformations and brain trauma (Castejón OJ. Invest Clin 26, 71-79, 1968; Castejón OJ. Invest Clin 28, 41-66, 1968; Castejón OJ. Invest Clin 29, 29-46, 1969; Castejón OJ. Anat Rec 163, 164, 1969; Castejón OJ. Anat Rec 166, 168, 1970; Castejón OJ. Invest Clin 38, 49-72, 1971; Castejón OJ, Castejón HV. Proc II Latin American Congress pp 34-35; pp 134-135, 1974; Castejón OJ, Castejón OC. Acta Cientif Venez (Suppl 1) 11, 1977; Castejón OJ. Acta Cientif Venez (Suppl 1)

16, 1977). These studies have been performed in pathological material such as cerebellar biopsies obtained during surgery. We have not included pictures of these studies in the present review because the edematous nature of the tissue and the distortion of cellular structures limit the comparison with the animal material processed for freeze-fracture SEM and freeze-etching technique.

Reviewer II: Does the author have a freeze-etching replica of the climbing fiber glomeruli to match figure 21?
Author: Not as yet.

Reviewer II: The beauty of Purkinje cells seems to disappear in SEM images (i.e., Fig. 26). Is it because you are dealing with human material or because of the ethanol-cryofracturing technique?
Author: The exposed surfaces of human cerebellar cells exhibited a shrunken aspect due to retraction induced by anoxic or postmortem changes in the autopsy material (Castejón and Valero, 1980). The possibility of artifactual changes such as freeze damage induced by the liquid nitrogen, mechanical deformation of the tissue at the time of fracturing and distortion caused by surface tension forces during critical point drying should also be considered. It is interesting to mention that ethanol-cryofracturing technique as applied by Humphreys et al. (1974, 1975) in normal liver tissue did not induce retracted changes or artifactual damage.

Reviewer III: The techniques thus far used for SEM of the hidden surfaces of the central nervous system are largely mechanical. Do you believe that further selectivity in microdissection might be achieved by chemical pretreatment (solubility, enzyme action, etc.)? Can you elaborate on this?
Author: Yes, indeed I believe that new reliable techniques and new rules of inference have to be established for further selectivity in microdissection. This subject was earlier raised by Zeeri and Lewis (Proc. 7º Congrés International de Microscopie Electronique. Grenoble, France, 1970. pp 481-482). Enzyme application (pronase, elastase, neuraminidase) or treatment with ethylenedinitrilo-tetraacetic acid (EDTA) can be assayed as chemical pretreatment. A mixture comprising 50% of 15mg pronase per cc of buffer and 50% of 10mg elastase per cc of buffer applied for twenty minutes is recommended by Zeeri and Lewis to remove neural sheaths in molluscs. A rather good success for exposing individual neurons and their processes has been reported by these authors with the application of 5mM of EDTA. It should be kept in mind that EDTA tends to dissolve connections among neurons, so a reliable study of neuronal circuits by Golgi method for light microscopy should be performed in advance of the SEM work. Further selectivity in microdissection might be achieved by using chondroitinase ABC, heparinase and neuraminidase, which digest the neuronal glycocalyx (Pease DC. J Ultrastruct Res 15, 555-588, 1966; Castejón HV. Acta Histochem 38, 55-64, 1970).